LIDAR FOR MAINTENANCE OF PAVEMENT REFLECTIVE MARKINGS AND RETROREFLECTIVE SIGNS

VOL II. RETROREFLECTIVE SIGNS

Final Report

PROJECT SPR-799

Oregon Department of Transportation

LIDAR FOR MAINTENANCE OF PAVEMENT REFLECTIVE MARKINGS AND RETROREFLECTIVE SIGNS

VOL II: RETROREFLECTIVE SIGNS

Final Report

PROJECT SPR799

by

Michael J. Olsen
Christopher Parrish
Erzhuo Che
Jaehoon Jung
Joseph Greenwood

for

Oregon Department of Transportation
Research Section
555 13th Street NE, Suite 1
Salem OR 97301

and

Federal Highway Administration
400 Seventh Street, SW
Washington, DC 20590-0003

October 2018

Technical Report Documentation Page

1. Report No. FHWA-OR-RD-19-03	2. Government Accession No.	3. Recipient's Catalog No.
4. Title and Subtitle LIDAR FOR MAINTENANCE OF PAVEMENT REFLECTIVE MARKINGS AND RETROREFLECTIVE SIGNS VOL II: RETROREFLECTIVE SIGNS		5. Report Date October 2018 6. Performing Organization Code
7. Author(s) Michael J. Olsen, Christopher E. Parrish, Erzhuo Che, Jaehoon Jung, and Joseph Greenwood		8. Performing Organization Report No.
9. Performing Organization Name and Address Oregon Department of Transportation Research Section 555 13th Street NE, Suite 1 Salem, OR 97301		10. Work Unit No. (TRAIS) 11. Contract or Grant No.
12. Sponsoring Agency Name and Address Oregon Dept. of Transportation Research Section 555 13th Street NE, Suite 1 Salem, OR 97301 Federal Highway Admin. 400 Seventh Street, SW Washington, DC 20590-0003		13. Type of Report and Period Covered Final Report 14. Sponsoring Agency Code
15. Supplementary Notes		

16. Abstract

Pavement markings and signs are important traffic control devices used to guide and regulate traffic movement through visual information presented to motorists. Signs and markings are made with retroreflective materials to enhance visibility for motorists, particularly at night. Retroreflectivity evaluation of an extensive highway network for maintenance and asset management purposes is a critical, yet challenging task for DOTs. Visual evaluation can often be subjective while field measurement techniques can be time-consuming and dangerous. This project investigated the effectiveness of evaluating pavement marking and sign retroreflectivity with mobile lidar data. Mobile lidar point clouds can be used to extract quantitative, accurate estimates of retroreflectivity for pavement markings, providing a safe, cost-effective, and reliable solution. Reliable retroreflectivity measurements of signs, however, was not possible due to sensor intensity saturation effects.

17. Key Words	18. Distribution Statement
Mobile lidar, retroreflectivity, pavement markings	Copies available from NTIS, and online at https://www.oregon.gov/ODOT/Programs/Pages/Research-Publications.aspx

19. Security Classification (of this report)	20. Security Classification (of this page)	21. No. of Pages	22. Price
Unclassified	Unclassified	XXX	

SI* (MODERN METRIC) CONVERSION FACTORS

APPROXIMATE CONVERSIONS TO SI UNITS

Symbol	When You Know	Multiply By	To Find	Symbol
		LENGTH		
in	inches	25.4	millimeters	mm
ft	feet	0.305	meters	m
yd	yards	0.914	meters	m
mi	miles	1.61	kilometers	km
		AREA		
in^2	square inches	645.2	millimeters squared	mm^2
ft^2	square feet	0.093	meters squared	m^2
yd^2	square yards	0.836	meters squared	m^2
ac	acres	0.405	hectares	ha
mi^2	square miles	2.59	kilometers squared	km^2
		VOLUME		
fl oz	fluid ounces	29.57	milliliters	ml
gal	gallons	3.785	liters	L
ft^3	cubic feet	0.028	meters cubed	m^3
yd^3	cubic yards	0.765	meters cubed	m^3
*NOTE: Volumes greater than 1000 L shall be shown in m^3.				
		MASS		
oz	ounces	28.35	grams	g
lb	pounds	0.454	kilograms	kg
T	short tons (2000 lb)	0.907	megagrams	Mg
		TEMPERATURE (exact)		
°F	Fahrenheit	(F-32)/1.8	Celsius	°C

APPROXIMATE CONVERSIONS FROM SI UNITS

Symbol	When You Know	Multiply By	To Find	Symbol
		LENGTH		
mm	millimeters	0.039	inches	in
m	meters	3.28	feet	ft
m	meters	1.09	yards	yd
km	kilometers	0.621	miles	mi
		AREA		
mm^2	millimeters squared	0.0016	square inches	in^2
m^2	meters squared	10.764	square feet	ft^2
m^2	meters squared	1.196	square yards	yd^2
ha	hectares	2.47	acres	ac
km^2	kilometers squared	0.386	square miles	mi^2
		VOLUME		
ml	milliliters	0.034	fluid ounces	fl oz
L	liters	0.264	gallons	gal
m^3	meters cubed	35.315	cubic feet	ft^3
m^3	meters cubed	1.308	cubic yards	yd^3
		MASS		
g	grams	0.035	ounces	oz
kg	kilograms	2.205	pounds	lb
Mg	megagrams	1.102	short tons (2000 lb)	T
		TEMPERATURE (exact)		
°C	Celsius	1.8C+32	Fahrenheit	°F

*SI is the symbol for the International System of Measurement

ACKNOWLEDGEMENTS

The authors thank the Oregon DOT Technical Advisory Committee for their assistance and valuable insight throughout this project. In particular, Jon Lazarus coordinated the overall research effort, Joel Fry helped facilitate and implement the logistics associated with the fieldwork, Lloyd Bledstoe acquired the mobile lidar data, and Dan Wright processed the mobile lidar data. Eric Leaming, Dennis Hackney, Nick Fortey, and Jason Motley also contributed feedback and insights throughout the project. We appreciate the assistance of Steve Barner, Meghan Jorgenson, and Shawn McKnight with the sign tests at the Oregon DOT maintenance yard. OSU students Nick Wilson, Nick Forfinski, Kory Kellum, Chase Simpson, Marian Jamieson, Katherine Shaefer, and Richie Slocum assisted with portions of the fieldwork. Leica Geosystems and David Evans and Associates provided equipment and software used in this research. Maptek I-Site provided software that was also used for this research. The authors also appreciate the efforts of Daniel Girardeau-Montaut and others in developing the open-source CloudCompare software used in this research.

DISCLAIMER

TABLE OF CONTENTS

LIST OF TABLES

LIST OF FIGURES

1.0 INTRODUCTION

Pavement markings and signs are important traffic control devices used to guide and regulate traffic movement through visual information presented to motorists. Signs and markings are made with retroreflective materials to enhance visibility for motorists, particularly at night. Retroreflectivity evaluation of an extensive highway network for maintenance and asset management purposes is a critical, yet challenging task for DOTs. Visual evaluation can often be subjective, while field measurement techniques can be time-consuming and dangerous. This project investigated whether mobile lidar datasets (georeferenced point clouds with intensity values and other attributes) could be used to extract quantitative, accurate estimates of retroreflectivity for pavement markings and signs, in order to provide a safe, cost-effective, and reliable method of performing these required evaluations.

Oregon DOT currently tracks several metrics for compliance of pavement markings, including appearance and retroreflectivity. The Maintenance & Operations Branch own a vehicle with a Laserlux 6 system, which travels the state every summer, to capture retroreflectivity values on lane markings. These readings are analyzed and used in creating a plan of action for maintenance (e.g., vendor replacement if covered under warranty, in house, or contracted maintenance). Unfortunately, issues arise due to the timing and frequency of the data acquisition. Often, individual hand-held reflectometer readings are required after winter months to recheck compliance, which may be risky (due to roadside work) and staff time intensive. Sign retroreflectivity evaluations suffer from similar limitations and are more cumbersome for crews.

Oregon DOT has been a national leader at the forefront of geospatial technologies such as mobile lidar. This technology supports a wide range of transportation applications (Olsen et al. 2013) within a single dataset that is acquired more safely and efficiently than conventional methods. Oregon DOT Geometronics is a unit within Oregon DOT and currently owns and operates a Leica Pegasus:Two, which is a survey-grade mobile lidar unit with two profilers to produce high-resolution point clouds. Oregon DOT Geometronics routinely scans Oregon DOT's highway network (on a two year cycle in dry conditions) to provide high quality geometric information along the highways to support a wide range of applications, particularly asset management. Mobile lidar systems provide intensity (return signal strength) data as a point attribute in georeferenced point clouds. These intensity values may be used in estimating retroreflectivity of pavement markings, which can be used for quality control purposes after construction or maintenance at a site or for statewide asset management to help meet performance goals by using the data that are already being collected and used by Oregon DOT for other purposes.

Recent research has investigated the potential use of mobile lidar for retroreflectivity evaluation (Olsen et al. 2013; Ai and Tsai 2016), primarily focused on signs. While the results of this work are promising, detailed studies were needed to assess the operational feasibility of these methods for state DOTs and to develop production-ready procedures. Research was performed to: a) develop and test operational procedures for generating retroreflectivity data from Oregon DOT's

mobile scanner, and b) evaluate the effects of challenging conditions, including precipitation, which are commonly encountered in the winter/spring seasons when crews evaluate lines for summer work. Since some aspects of the lidar radiometric (intensity) calibration are specific to a particular system and configuration, it was critical to modify and test these procedures using data directly from Oregon DOT's system.

1.1 OBJECTIVES

SPR799 Lidar for Maintenance of Pavement Reflective Markings and Retroreflective Signs Vol II: Retroreflective Signs has the following research overarching objectives:

- Develop a model for retroreflectivity and radiometric calibration for Oregon DOT's mobile lidar system.
- Generate a set of quality control metrics for pavement marking and sign retroreflectivity based on information derived from mobile lidar data.
- Establish procedures for extracting road markings from lidar data and creating GIS data layers from the output of the above steps to support decision making by supervisors and integrate analysis results into Oregon DOT's overall workflows.

This final report summarizes several research tasks performed to accomplish these research objectives, including describing the field experiments, the radiometric calibration procedure, the validation process, the development of striping and sign quality control metrics, and ultimately, the integration of the results into an efficient GIS tool. The final report is split between two volumes. Volume I of the report focuses on pavement markings; whereas Volume II (this volume) focuses on signs. Volume II documents the findings (including the limitations noted) and is intended to serve as a helpful reference, should ODOT pursue sign retroreflectivity evaluation with a future mobile lidar system. There are several examples found in the literature of successful usage of mobile lidar for sign retroreflectivity evaluation.

A key finding of this research is that, while mobile lidar is effective for evaluation of retroreflectivity of pavement markings (Volume I); it is significantly less so for evaluation of retroreflectivity of signs (Volume II). Primary factors include: 1) readings on signs are collected at low (orthogonal) angles of incidence (as compared with measurements on pavement markings, which are at more oblique angles); 2) many types of sign sheeting provide very high levels of retroreflectivity (meaning that even at high incidence angles (oblique), saturation of returned lidar signals can still occur); and 3) it is a difficult optical design challenge for mobile lidar systems to achieve a dynamic range sufficient to cover both dark (low-reflectance) targets such as the pavement surface and extremely high retroreflective targets. Mobile lidar systems are often designed to focus on the objects with lower reflectivity since those comprise the overwhelming majority of the natural and built environment. As a result of the combination of these factors, lidar intensity values from ODOT's current mobile scanner (Leica Pegasus: Two) obtained on retroreflective signs were found to typically be saturated (beyond the upper limit of the system's measurement range) in this research. Unfortunately, it is impossible to extract meaningful information from saturated intensity readings, as the measurements are effectively

"chopped off" during acquisition, and hence no amount of post-processing can recover the correct values.

1.2 ORGANIZATION OF REPORT

This report is divided into two volumes. Volume I explores and develops the capabilities of using mobile lidar for evaluating reflective pavement markings while Volume II (this volume) explores the feasibility of using mobile lidar for evaluating retroreflective signs.

Volume II is organized as follows:

Chapter 2 provides a detailed literature review, which evaluates the current state-of-the-art methodologies for retroreflectivity measurements for signs with their associated advantages and disadvantages. In particular, the review focuses on the utility of mobile lidar systems for extracting retroreflective measurements on signs. Successful examples of utilizing mobile lidar for this purpose were found in the literature.

Chapters 3 describes preliminary sign evaluation tests completed at the ODOT Testdeck located near Stayton, OR. This test was primarily focused on pavement marking evaluation. A series of mobile lidar scans were captured in different scanning configurations, lanes, and speeds in order to provide a comprehensive dataset to develop a radiometric calibration.

Chapter 4 summarizes the performance of the mobile lidar unit for capturing signs. A more rigorous test is conducted, focused on evaluating whether the mobile lidar system is capable of obtaining valid retroreflective readings on signs that were at the failing point considering a variety of geometric configurations. Unfortunately, for the reasons noted above, the intensity readings were typically found to be saturated (even on the failing signs) and, therefore, unusable for subsequent processing and analysis for sign retroreflectivity analysis.

Chapter 5 provides conclusions, summarizing key findings of this research. It also discusses the limitations of the work and recommendations for future research and development.

2.0 LITERATURE REVIEW

2.1 OVERVIEW

This chapter presents a comprehensive literature review to evaluate the current state-of-the-art methodologies for retroreflectivity measurements for signs with their associated advantages and disadvantages. In particular, the review will focus on the utility of mobile lidar systems for extracting these measurements.

The literature review starts with a brief background on the physics underlying retroreflectivity. The section describes current procedures and reference manuals for obtaining reliable retroreflectivity readings. The review then describes mobile lidar technology, including a brief history of mobile lidar usage within Oregon DOT. Following the background, critical concepts are covered related to lidar intensity (return signal strength) and radiometric calibration principles. For more detailed information on radiometric calibration procedures, a recently published review of current radiometric calibration procedures has been published in Kashani et al. (2015). The next two subsections discuss current research utilizing mobile lidar data for retroreflective readings as well as sign feature extraction techniques. Finally, the chapter closes with a description of challenges and possibilities, which were helpful guiding the work completed on SPR-799 and may be useful to future research efforts.

2.2 RETROREFLECTIVITY BASICS

When propagating electromagnetic radiation (such as the light from a vehicle's headlights) encounters a surface, it can be reflected, absorbed, and/or transmitted in varying proportion. From the law of conservation of energy, the fractions of the light transmitted, absorbed and reflected must sum to one, or:

$$\boldsymbol{\tau + \alpha + \rho = 1} \tag{2-1}$$

Where:

$$\boldsymbol{\tau = \frac{E_t}{E_i};\ \alpha = \frac{E_a}{E_i}\ ;\ \rho = \frac{E_r}{E_i}} \tag{2-2}$$

In Eq. 2-2, E_i is the incident energy, and E_t, E_a, and E_r, are, respectively, the transmitted, absorbed and reflected energies. The quantity, ρ, is referred to as reflectance, a measure of how well a surface reflects incident radiant energy. More specifically, it is the so-called "bi-hemispherical" reflectance, as it assumes diffuse illumination and reflection over all viewing angles. In the more general case, it is of interest to model reflectance as a function of the viewing

and illuminating geometries. This can be achieved using a bidirectional reflectance distribution function (BRDF), which is a function of four variables: two describing the direction of the illumination source relative to the surface normal, and two describing the direction of the viewer (i.e., the person, camera or sensor receiving the reflected light) (Jensen 2005; Schaepman-Strub et al. 2006).

Three special, or ideal, cases of reflection can be defined (Austin and Schultz 2009):

- Perfect specular reflection
- Perfect diffuse reflection
- Retroreflection

Specular reflection arises from a very smooth surface (relative to the wavelength of the light), and results in light being reflected away from the illumination source, with the angle of reflection being equal and opposite the angle of incidence (Figure 2.1a). Mirror-like and metal surfaces (often described as being "shiny" in appearance) exhibit specular reflection. Diffuse reflection is the opposite case from specular, and involves a surface reflecting light equally well in all directions (Figure 2.1b). Rough surfaces, which are often described as appearing "flat or matte," are diffuse reflectors. The third special case is retroreflection, in which light is reflected back in the direction of the illumination source (Figure 2.1c). This type of reflection is typically achieved through corner cube reflectors or glass beads, which are specifically designed for this purpose (Lloyd 2008; Burns et al, 2008).

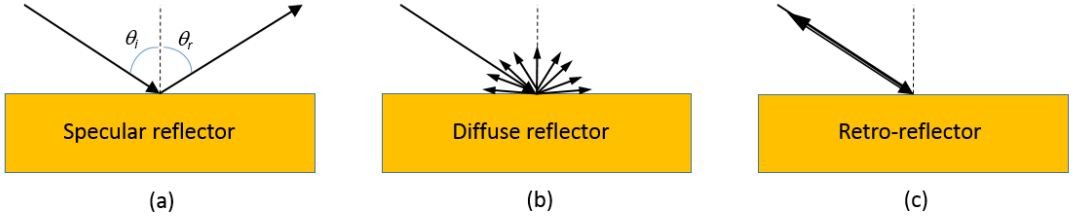

Figure 2.1: Three special cases of reflection: (a) specular, (b) diffuse, and (c) retroreflection.

Retroreflection plays an important role in increasing nighttime visibility of traffic signs and pavement markings. Specifically, if signs and pavement markings are designed to reflect light from a vehicle's headlights back to the driver, this increases the distances from which the pavement markings and signs can be seen at night and improves clarity (Austin and Schultz 2009). Statistics on the significantly higher fatal crash rates at nighttime, as compared with daytime, are frequently cited as an indication of the importance of retroreflectivity (FHWA 2009). At least as far back as the 1930s and the publication of the first version of the Manual on Uniform Traffic Control Devices (MUTCD), it was recognized that sign retroreflectivity was important to highway safety and efficiency (Carlson and Hawkins 2003). The late 1930s also saw the release of the first commercial enclosed bead sheeting (Lloyd 2008). The 1993

Department of Transportation Appropriations Act (Public Law 102-388) mandated that the MUTCD be revised to establish minimum maintained levels for retroreflectivity for signs (McGee and Taori 1998; Carlson et al. 2003), and these minimum retroreflectivity (MR) levels are specified in Table 2A–3 of the current MUTCD 2009 Rev 2 (FHWA, 2012).

Luminance is the photometric quantity describing the amount of light reflected, emitted or traveling through a given area and within a given solid angle, and is given in units of candela per square meter (cd/m^2). Loosely defined, luminance is a measure of how bright a surface appears to an observer viewing the surface from a particular angle. The ratio of luminous intensity to illuminance (the luminous flux incident on a surface per unit area in units of lux) provides a measure of retroreflectivity. In particular, retroreflectivity is typically reported in terms of retroreflected luminance, R_L, in units of candelas per lux per square meter ($cd/lx/m^2$) or millicandelas per lux per square meter ($mcd/lx/m^2$) (Migletz et al. 1999). Minimum retroreflectivity levels specified in MUTCD 2009 Rev 2. Table 2A-3 are given in $cd/lx/m^2$ measured at an observation angle of 0.2° and an entrance angle of ~4.0°.

Retroreflective sheeting used on traffic signs is classified into various types, which are specified in the American Society for Testing and Materials (ASTM) specification D4956: "Standard Specification for Retroreflective Sheeting for Traffic Control" (ASTM International 2016). Types I through III are beaded sheeting, while IV through X are prismatic sheeting. Some of the types are also referred to by other terms: for example, Type I is referred to as "engineering grade," while Type V is "super high-intensity."

In addition to signs, pavement markings are another type of traffic control device that make use of retroreflectivity. In the case of pavement marking materials (PMM), retroreflectivity is typically achieved through the use of glass beads or microspheres embedded in the paint (Austin and Schultz 2009). Other types of marking materials include waterborne paint, epoxy, polyester, thermoplastic, and tape (Migletz et al. 1999). Advanced types of PMM have been shown to enable savings in pavement marking budgets in various state DOTs (Saetern 2016).

Unfortunately, the retroreflectivity of traffic control devices degrade over time, as a function of traffic, weather, orientation, and precipitation, among other variables (Kirk et al. 2001; Migletz et al. 1999). It is for this reason that policies and procedures are in place to assess and maintain retroreflectivity over time. The specific wording in the MUTCD 2009 Rev. 2 is:

> *Public agencies or officials having jurisdiction shall use an assessment or management method that is designed to maintain sign retroreflectivity at or above the minimum levels in Table 2A-3.*

Since degraded retroreflectivity can adversely affect safety, while premature replacement of signs and pavement markings can unnecessarily increase costs, effective inspection and maintenance procedures are critical to state DOTs. Current inspection methodologies fall into two general types: 1) a visual nighttime inspection using human inspectors, and 2) quantitative measurements made with retroreflectometers (Figure 2.2). Policies of blanket replacement on a set schedule may also be followed, but the disadvantage is wasted cost of unnecessary replacement of some signs (Austin and Schultz 2009).

Figure 2.2: Retroreflectometer being used to measure retroreflectance of a stop sign (Figure from FHWA: https://safety.fhwa.dot.gov/local_rural/training/fhwasa09025/fhwasa09025.pdf).

2.2.1 Degradation of retroreflectivity in wet conditions

Retroreflectivity can be significantly reduced when the surface is wet, such as during or just after a period of rainfall (Schnell et al. 2003; Lundkvist and Isacsson 2007; Carlson et al. 2007). One of the primary causes of this reduction in retroreflectivity is specular or "mirror-like" reflection (see Figure 2.1a) from a surface covered by a film of water, which leads to light from the headlights being reflected off in a direction away from the driver, rather than back towards the driver (Schnell et al. 2003; Pike et al. 2007). Refraction (bending) of the light rays at the air-water interface alters the optical path and can also lead to a reduction in retroreflectivity (Pike et al., 2007; Carlson et al. 2007; Burns et al. 2008). The effect of a layer of water on a bead can be modeled as an effective change in the refractive index of the bead (Burns et al. 2008). In pooled water, light can also be scattered and absorbed within the water column, further reducing the proportion of incident light reflected back toward the driver.

There is some evidence to suggest that it may be possible to establish simple mathematical relationships between retroreflectivity under wet and dry conditions (Lundkvist and Isacsson 2007), indicating the potential to predict retroreflectivity under wet conditions from measurements in dry conditions, or vice versa. However, additional research is needed to develop and test such prediction methods and to determine the ranges of conditions and marking types under which they will hold. It should also be noted that "all weather" retroreflective materials that make use of multiple types of beads are now available from commercial manufacturers, but their performance and durability is still an active area of research (e.g., Hawkins et al. 2015).

2.3 NATIONAL STANDARDS AND METHODOLOGIES

A variety of standards and specifications have been developed by ASTM, AASHTO, DOTs, TRB, and other organizations for evaluating pavement retroreflectivity. This section will briefly summarize the most relevant procedures to SPR799.

The MUTCD 2009 Rev. 2 requires public entities to have an assessment or management method in place to ensure sign retroreflectivity at or above minimum levels for regulatory and warning signs. This section will describe each of the recommended approaches in the manual. Table 2.1 presents the minimum sign maintained retroreflectivity values in Table A.3 in the MUTCD 2009 Rev. 2. Several approaches are recommended and are summarized in the following subsections (2.3.2.1-2.3.2.7).

Table 2.1: MUTCD 2009 Rev. 2. Minimum Maintained Retroreflectivity Values (from MUTCD 2009 Rev. 2 Table A.3).

Color	Sheeting Type (ASTM D4956-04)				Additional Criteria
	Beaded Sheeting			Prismatic Sheeting	
	I	II	III	III, IV, VI, VII, VIII, IX, X	
White on Green	W*; G ≥ 7	W*; G ≥ 15	W*; G ≥ 25	W ≥ 250; G ≥ 25	Overhead
	W*; G ≥ 7	W ≥ 120; G ≥ 15			Ground-mounted
Black on Yellow/ Black on Orange	Y*; O*	Y ≥ 50; O ≥ 50			(2)
	Y*; O*	Y ≥ 75; O ≥ 75			(3)
White on Red	W ≥ 35; R ≥ 7				(4)
Black on White	W ≥ 50				—

1. The minimum maintained retroreflectivity levels shown in this table are in units of cd/lx/m^2 measured at an observation angle of 0.2° and an entrance angle of -4.0°.
2. For text and fine symbol signs measuring at least 1200 mm (48 inches) and for all sizes of bold symbol signs.
3. For text and fine symbol signs measuring less than 1200 mm (48 inches).
4. Minimum Sign Contrast Ratio ≥ 3:1 (white retroreflectivity ÷ red retroreflectivity).
URL reference: https://safety.fhwa.dot.gov/roadway_dept/night_visib/policy_guide/fhwasa07020/
* This sheeting type should not be used for this color for this application.

The MUTCD 2009 Rev. 2 also specifies special cases such as:

- W3-1 – Stop Ahead: Red retroreflectivity ≥ 7
- W3-2 – Yield Ahead: Red retroreflectivity ≥ 7; White retroreflectivity ≥ 35

- W3-3 – Signal Ahead: Red retroreflectivity ≥ 7; Green retroreflectivity ≥ 7
- W3-5 – Speed Reduction: White retroreflectivity ≥ 50
- For non-diamond shaped signs such W14-3 (No Passing Zone), W4-4p (Cross Traffic Does Not Stop), or W13-1, -2, -3, -5 (Speed Advisory Plaques), use largest sign dimension to determine proper minimum retroreflectivity level.

2.3.1 Visual Nighttime Inspection (VNI)

Three forms of visual nighttime inspection are typically implemented.

- ***Comparison Panel*** - An observer/inspector evaluates the quality of a sign at night time. A comparison panel (that has been tested for retroreflectivity at or slightly above the minimum required retroreflectivity) is attached to the sign and the inspector rates the condition of the sign.
- ***Calibration Sign*** – The trained inspector initially calibrates their eyes to sample signs that are near the minimum retroreflectivity requirement each night prior to assessing the signs in their routes.
- ***Consistent Parameter*** - An inspector who is at least 60 years old and rides in an SUV or truck with a model year newer than 2000 based on FHWA requirements. The inspection is completed at night (complete darkness) and low intensity beams are used. The vehicle travels at highway speeds and the inspector rates the signs.

2.3.2 Measured Sign Retroreflective readings

Handheld retroreflectometers are used to obtain readings across a sign. The following ASTM reference provides procedures for measuring sign retroreflectivity:

- ASTM E1709 Standard Test Method for Measurement of Retroreflective signs using a Portable Retroreflectometer.

Specifically, measurements are to be obtained at several locations across the sign. The devices are based on a specific geometry with an entrance angle of -4.0° and an observation angle of 0.2°. Typically, at least 4 measurements are completed. Measurements must be taken and averaged for 0° and 90° orientation using a point instrument (single light detector) since some sheeting shows differences based on the orientation. However, an annular instrument that has a circular light detector does not require this averaging. The instruments are calibrated to 321 cd/lx/m^2. Readings should be obtained on the background and the legend. The operator should document sign location, sheeting type, and the overall test results. Acceptable readings depend on the type of sheeting material as defined by ASTM D4956. Recently, AASHTO (2015) has updated these classifications of sheeting material and provides minimum coefficients of retroreflection:

- AASHTO M268. Standard Specification for Retroreflective Sheeting for Flat and Vertical Traffic Control Applications

AASHTO M268 also considers a wider range of entrance and observation angles.

Several challenges exist in acquiring reliable retroreflective measurements using these portable devices. Users must be trained in their usage and perform regular calibrations. They also must have direct access to the signs, requiring equipment such as ladders. For large overhead signs, this can present several logistical and safety concerns. Dirty signs can also be problematic.

Some mobile platforms also exist for efficiency and safety enhancements; however, they currently struggle with reliable readings. Many of these systems were evaluated through the FHWA Strategic Highway Research Program (SHRP) 2 S-03 Rodeo held in Sept. 2008 and at the time were unsuccessful at producing reliable results (Hunt et al., 2011).

2.3.3 Expected Sign Life

Signs may be replaced at a fixed interval of time in service. The installation date is recorded and the sign is labeled. This approach is based on limited empirical data of the performance of signs in the area. Given the logistical difficulties in frequently obtaining retroreflective readings, isolating specific signs for replacement, some DOTs have found it more efficient to replace signs based on their expected life.

2.3.4 Blanket Replacement

Another strategy is to replace all signs in an area at the same time. This approach does not require sending personnel to the field to obtain retroreflective readings on signs, reducing labor costs. An advantage to this approach is that an agency can more easily plan for and manage the replacement of signs. The agency does not need to track and manage much of the monitoring data required in the other approaches. A disadvantage is that a number of signs that still meet requirements are removed unnecessarily from service, so there is a higher cost associated with the maintenance labor and physical costs of frequency replacing the signs.

Some DOTs, counties, and cities have started a recycling and refurbishment program to reduce costs, as opposed to complete replacement. Past efforts at ODOT have included these recycling efforts, which resulted in additional sign monitoring for those that were refurbished to determine lifespan (Lazarus, 2012). It is too early to tell if refurbished signs have the same lifespan as newly sheeted signs.

2.3.5 Control Signs

Specific signs are designated as control signs and monitored to determine when to replace the other signs in the area, typically through a blanket replacement approach. The condition of these signs are regularly monitored. When the control signs approach the minimum retroreflectivity levels, then the signs in the area are replaced.

2.3.6 Future Methods Based on Engineering Study

The MUTCD 2009 Rev. 2 allows for a DOT to develop their own methods provided that they have a supporting study.

2.3.7 Combinations

Combinations of the above approaches are also permitted and are often implemented.

2.3.8 Implementation

NCHRP Synthesis 431 surveyed multiple DOTs and local agencies in 2011. Of those surveyed, most were not measuring retroreflectivity, but rather, were using either expected sign life, nighttime inspection, or blanket replacement as their primary means for determining sign replacement. Many were using expected sign life or control signs as their secondary indicator.

A similar study by AASHTO in 2014 found similar results to NCHRP Synthesis 431. Night inspection intervals were typically 1-3 years, and expected service life/blanket replacement intervals varied between 10-17 years.

2.3.9 Additional Considerations

Other metrics of interest besides retroreflectivity for signage include the orientation of the sign to the roadway, contrast of retroreflectivity between the text and sign background, obstruction by vegetation, and many other factors.

2.4 OREGON DOT PROCEDURES

Oregon DOT has developed internal procedures and policies for sign maintenance and replacement. Note that these procedures are updated regularly and one of the purposes of SPR-799 is to inform future updates to these procedures. This section will briefly summarize relevant documents.

2.4.1 Maintenance protocols

Maintenance protocols related to retroreflective signs are provided in "*Desired Conditions of Maintenance Features on State Highways*" (Oregon DOT 2002). This document provides objective descriptions of desired conditions for highway features to optimize use of tax dollars. It provides a system of five level-of-service ratings (A-E) to describe the feature's condition. Table 2.2 summarizes the desired condition for level of service of signs.

2.4.2 Design Manual

Traffic sign design protocols are found in the ODOT *Traffic Sign Design Manual* (Oregon DOT 2018). This document estimates that the typical service life of a sign ranges from 10-17 years. When performing a project, the manual suggests considering replacement of signs that are close to the end of their lifespan.

2.4.3 Inventory protocols

Inventory protocols related to signs can be found in the following:

- *ODOT Sign Inventory Database User's Guide* (Oregon DOT 2013a) provides instructions for performing basic sign inventory data collection in a standardized format. It describes the components of the database, key information to collect, and protocols for entering that information into the database.

- *ODOT Sign Inventory Database Field Handbook Guide* (Oregon DOT 2013b) is the accompanying field manual that provides instructions to field crews on data collection as well as critical reference information for the field crew.

2.4.4 Warranty specifications

General ODOT warranty specifications are covered in:

- Section 00170.85(c)(1), Responsibility for Defective Work of Part 00100, General Conditions, in the Oregon Standard Specifications for Construction. (Oregon DOT 2015a).

Table 2.2: ODOT Desired Conditions Level of Service Requirements for Street Signs

Level of Service	Surface material condition	Geometric condition	Posts	% Illumination Working	Response time (Critical regulatory and warning)	Response time (Non-safety regulatory and warning and directional)
A	No peeling, fading, or scratches visible	All signs at correct height or placement	Drilled wooden posts for crash worthiness	100, readable day and night		
B	Little peeling, minor fading, minor scratches	All signs at correct height or placement	Drilled wooden posts for crash worthiness	90	2 hours	1-2 days
C	Some peeling, evidence of dead spots	Few signs not at correct height or placement	Drilled wooden posts for crash worthiness	80	2-3 hours	2-4 days
D	Definite peeling or dead spots, significantly faded, or scratched	Most signs at correct height or placement. Some signs noticeably lean	Only a few wooden posts have not been drilled.	50	> 3 hours	> 4 days
E	Illegible due to peeling, dead spots, fading, cracking.	Most signs lean significantly, many signs are not at correct height or placement	Some wooden posts have not been drilled.	<50	>3 hours	> 4 days

2.4.5 Prior Research on Sign Retroreflectivity

Previously, a research project was completed in 2001 (*Kirk et al. 2001*) by ODOT to evaluate factors affecting sign retroreflectivity, with a focus on age and physical orientation to guide ODOT's management of road signs. Interestingly, over a 12 year span, most signs still

maintained retroreflectivity readings above the minimum ODOT standards. They also found some evidence that sign retroreflectivity may sometimes be influenced by sign orientation due to weathering effects such as windblown dust and precipitation; however, more studies were needed to provide more evidence. Lazarus et al. (2012) researched the benefits of aluminum sign recycling programs and evaluated whether recycled signs could meet ODOT specifications.

2.5 MOBILE LIDAR TECHNOLOGY

Mobile lidar (ML, also called Mobile Laser Scanning, MLS, or Mobile Terrestrial Laser Scanning, MTLS), hereafter referred to as MTLS, systems can acquire detailed 3D data efficiently from a moving vehicle at highway speeds with traffic. Georeferencing (i.e., the assignment of precise, 3D spatial coordinates in a defined coordinate system to each point in a lidar point cloud) can be completed directly with the combination of components included on the scanner (e.g., GNSS-aided inertial navigation systems); however, for highest accuracy applications, rigorous survey control points are often established. In addition to a wealth of geometric information across the roadway and surrounding area, a key benefit to mobile lidar data is its intensity information, which is related to the reflectivity of the objects.

Lidar provides several benefits and, as a result, is being widely adopted by DOTs across the country (*NCHRP Report 748* and *NCHRP Synthesis 446*). One of the key benefits of lidar is the fact that the same lidar dataset can be used by multiple people for a wide variety of applications, minimizing the need for multiple data collects. This versatility has resulted in the phrase, "*Collect once, use many times*" when discussing lidar. Figure 2.3 presents a sampling of these applications in transportation.

Additionally, one can remotely survey a site from safe locations, minimizing the danger to field crews and the travelling public. Lidar also enables a much more efficient and thorough field survey, minimizing the need for costly repeat visits to the site to collect information. The reduction in field time and ability to acquire data from the sides of the road with static lidar or at traffic speeds with mobile lidar provides significant safety benefits over typical surveying.

The comprehensive information provided by lidar greatly improves the detail in models used throughout the design process and, hence, reduces uncertainty in decision-making. The additional information that is resolvable in lidar data enables topography and other features to be modeled at a higher level of detail and accuracy over traditional techniques. This detailed, 3D virtual world provides personnel in the transportation agency with a much better understanding of the field conditions and variability throughout the site.

Another key benefit of mobile lidar is the ability to integrate other sensors onto a single mobile platform (*NCHRP Synthesis 446*). This enables the collection of a wide variety of important metrics needed for various applications from a single data collection effort.

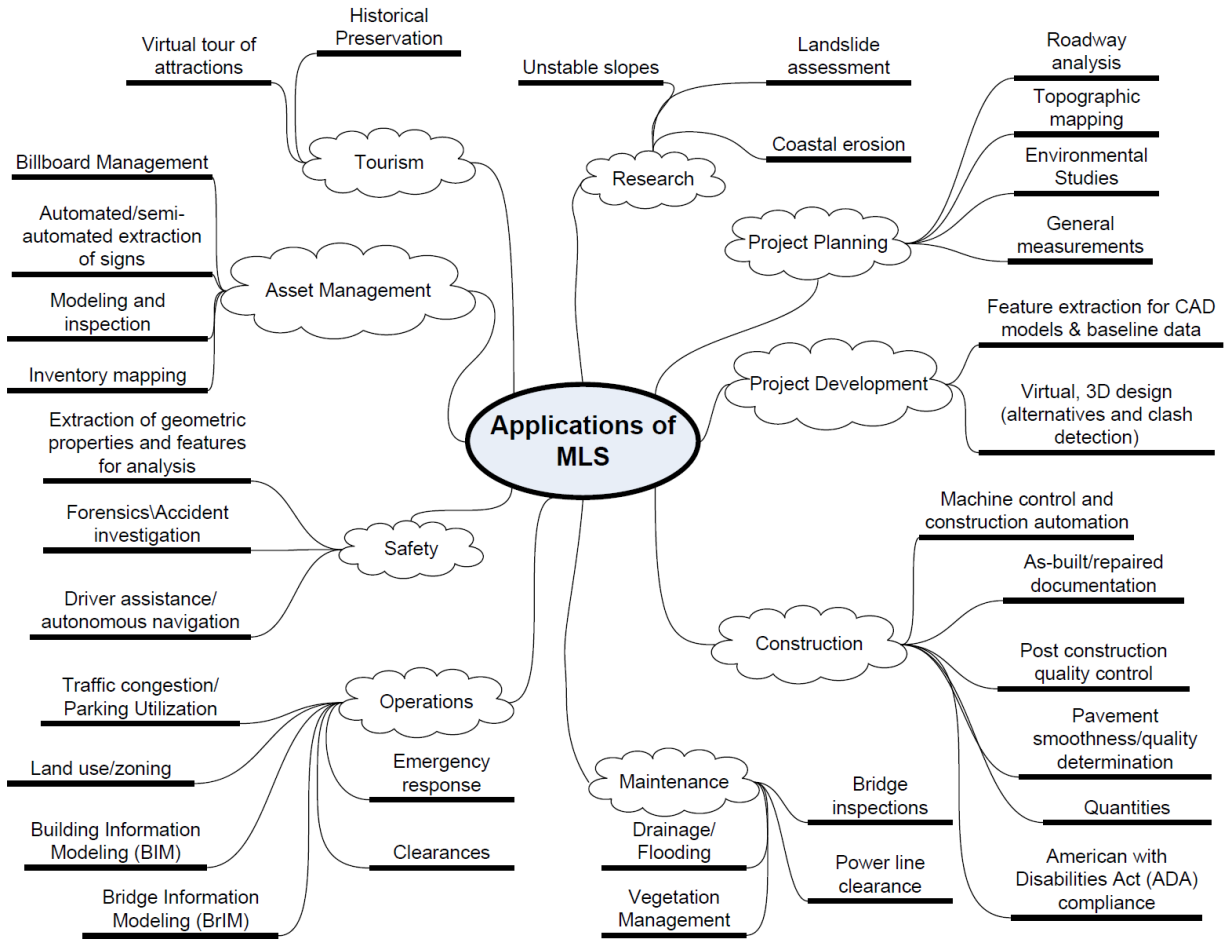

Figure 2.3: Sample applications using mobile lidar technology in transportation. From NCHRP Report 748

A wide range of MTLS systems exist depending on the scope of the survey. Puente et al. (2013) describes and compares configurations of a variety of MTLS. Systems can be designed to be specialized for certain applications such as pavement analysis or configured for general data acquisition. Lower cost asset management & mapping systems (~$400k) can achieve sub-meter (<3.3 ft) accuracies at the network level and decimeter (several inches) accuracies at the local level. Survey grade systems (~$1 million) can achieve centimeter (<1in) level accuracies at both the network and local level. While highest accuracy has required the use of dense targets, higher accuracy and more reliable results can be obtained by performing multiple passes of a section, enabling improved verification of Global Navigation Satellite System (GNSS) quality as well as trajectory enhancements by averaging multiple passes (Nolan et al. 2015a; 2015b).

One of the first DOTs to develop formal specifications was Caltrans (Chapter 15 California Survey Manual). These specifications have been modified and adopted by other DOTs such as Florida DOT. Caltrans has continued to develop best practices, workflow, and training documentation for mobile laser scanning data collection (Yen et al. 2014).

NCHRP Report 748 provides performance-based guidelines for the use of mobile lidar in transportation applications (Olsen et al. 2013c). Based on interviews with state DOTs and service providers, the report indicates that transportation agencies have a strong interest in mobile lidar going forward, but there are very few examples of best practices and/or in-depth discussions of results. This guideline establishes nine data collection categories (DCC) that are appropriate for the specific transportation applications based on resolution and accuracy requirements. The guidelines also provide general recommendations concerning the critical issue of data management. It is divided into two main sections: Management and Technical. The management portion contains a discussion of applications, workflows, data mining, procurement process, decision making, an implementation plan, and currently available guidelines. The technical section describes the components of MTLS, error sources, calibration and correction, accuracy and resolution requirements and specification, quality control methods, considerations for common applications, information management, deliverable specification, and future trends. Appendices also contain sample calibration reports and templates for developing scopes of work. This work was developed into an e-learning website (https://learnmobilelidar.com), which includes online, interactive learning modules, a detailed and searchable reference list, and user forums to help educate about mobile lidar usage to support transportation applications.

2.5.1 Mobile lidar at Oregon DOT

Oregon DOT has been an early adopter of mobile lidar technology. When the technology first became available, Oregon DOT contracted its use on several highway projects. In 2011, Oregon DOT purchased at TopCon IPS2 mobile lidar system primarily for asset management purposes. To the authors' knowledge, Oregon DOT was the first state DOT to own a mobile lidar system in 2011. Data from mobile lidar surveys were used to extract features to update asset management databases. As more people within Oregon DOT started utilizing the data, additional applications were identified, such as the use of the mobile lidar scans to measure drive approaches.

After several years working with and becoming more comfortable with the technology, Oregon DOT purchased a survey-grade system, the Leica Pegasus:Two (Figure 2.4Figure 2.4). The higher quality of the data enables it to be used for a broader range of applications. This system also is a versatile system that can be mounted on additional vehicles aside from a truck or SUV such as ATVs or boats for more difficult to reach locales. The system also includes 8 cameras (7 providing a panoramic view and one focused on the pavement), enabling it to provide a detailed video log of the highway in addition to the geometric information provided by the scanner.

Oregon DOT's Engineering Technology Advancement (ETA) group is currently exploring additional opportunities to utilize the mobile lidar system throughout Oregon DOT to either complement or replace current data collection procedures. Current activities with mobile lidar at Oregon DOT are described on their webpage: (https://www.oregon.gov/ODOT/HWY/ETA/Pages/Mobile-LiDAR-Applicaitons.aspx). Oregon DOT's mobile lidar system is being utilized for acquiring survey data for project development, measuring vertical clearances, asset management, pavement evaluation, slope stability monitoring, accident reconstruction, and many more.

Figure 2.4: Oregon DOT's current mobile lidar system, Leica Pegasus:Two.

Recently, Oregon raised the speed limit on the state Highways in central and eastern Oregon. This project required Oregon DOT to evaluate sight distance as well as passing zone striping with the increased speed to ensure that they would be compliant with safety regulations. Mobile lidar data already collected from Oregon DOT's routine mapping were extensively used in the supporting passing distance studies. These data ensured that Oregon DOT could complete the necessary remediation quickly to meet strict timelines (Oregon DOT, 2015).

Oregon DOTs vision is to utilize mobile lidar and other technologies to provide a real-time, digital transportation system (Singh et al. 2009). When construction projects or maintenance is completed, the data would be updated to reflect those changes.

2.5.2 Intensity and Radiometric Calibration

Intensity values are often provided with lidar data sets as an additional attribute to accompany the X,Y,Z spatial coordinates of points and color information (Figure 2.5 top). These intensity values are a measure of backscattered signal strength and contain information on surface characteristics, including reflectance (Figure 2.5 bottom). However, the raw intensity values are generally provided as uncalibrated digital numbers, and, in addition to surface reflectance at the laser wavelength, they are also a function of several extraneous variables related to the environment, system and acquisition parameters (Höfle and Pfeifer, 2007; Wagner et al., 2008; Kaasalainen et al., 2009; Jutzi and Gross, 2009; Vain et al., 2009). Examples of these extraneous variables include laser range, incidence angle, receiver aperture, system transmittance, atmospheric transmittance, beam divergence, and transmitted laser power.

A great number of lidar intensity correction and radiometric calibration procedures have been developed with the goal of removing the effects of these environmental and system variables to provide values that better represent surface reflectance. (As a side note on terminology, while some authors draw a distinction between reflectance and reflectivity based on surface type, the terms are used interchangeably here.) Depending on the level and type of correction, the output may be referred to as calibrated intensity, pseudo-reflectance, relative-reflectance, reflectance factor, or true surface reflectance.

Kashani et al. (2015) provide a comprehensive review of different methods of radiometric calibration and correction and classify them into the following general processing levels:

- Level 0: Raw intensity (no correction)
- Level 1: Intensity correction
- Level 2: Intensity normalization
- Level 3: Rigorous radiometric calibration

Based on the Kashani et al. (2015) classification of intensity correction/calibration, examples of work using Level 1 processing include Luzum et al. (2004), Jutzi and Gross (2009), and Korpela et al. (2010) while Level 3 processing is discussed in Ahokas et al. (2006), Kaasalainen et al. (2009), and Briese et al. (2012).

Another method of classifying radiometric processing strategies discussed in Kashani et al. (2015) is to separate them into: 1) theoretical or model-driven approaches, and 2) empirical approaches. Those in the first category generally involve inverting the laser range equation to obtain surface reflectance as a function of (known, modeled, or assumed) system, acquisition and environmental variables. Although many different forms of the laser range equation have been published (e.g., Jelalian 1992; Baltsavias 1999; Höfle and Pfeifer 2007; Wagner et al. 2008; Mallet and Bretar 2009; Kaasalainen et al. 2011), a common form—under the assumption of a Lambertian, area target—is:

$$\boldsymbol{P_r = \frac{P_t D_r^2 \eta_{atm} \eta_{sys} \rho}{4R^2} \cos \theta_i} \qquad \textbf{(2-3)}$$

Where:

P_r = received optical power (watts), P_t = transmitted power (watts), D_r = receiver aperture diameter (meters), η_{atm} = atmospheric transmission factor (dimensionless), η_{sys} = system transmission factor (dimensionless), ρ = target reflectance at the laser wavelength (dimensionless), R = range (meters), and θ_i = incidence angle. Empirical approaches are generally similar, but rely largely on experimentally estimated parameters, rather than mathematical models.

Because the transmitter and receiver in a lidar system are collocated as closely as possible, lidar intensity inherently measures something akin to retroreflectivity (i.e., the amount of laser light reflected *back in the direction of the source*.) In fact, if lidar intensity data can be appropriately corrected—using, as a basis, the methods presented in the work referenced here—they can provide good estimates of surface retroreflectivity. It is this observation that forms the theoretical basis for this work.

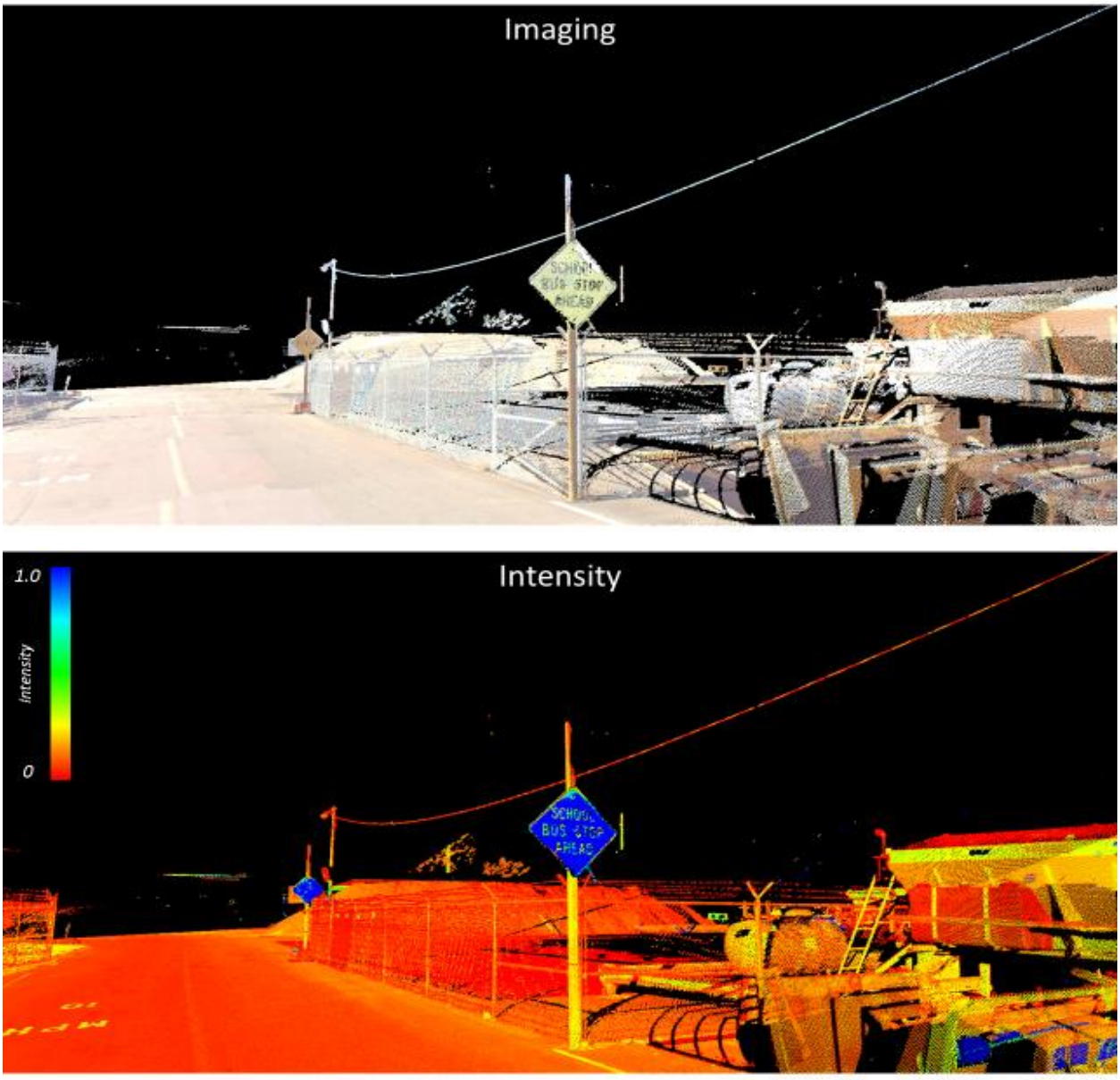

Figure 2.5: Mobile lidar data collected by ODOT at an ODOT Maintenance Yard during the sign test. In the top image, the point cloud data are colored by the images collected by the cameras mounted on the mobile lidar system. In the bottom image, the same point cloud is shown displayed by intensity. Although the intensities shown here are un-calibrated, the "SCHOOL BUS STOP AHEAD" sign is recognizable due to the contrast of intensity values.

2.5.3 Quality control measurements from lidar

Several studies evaluate the geometric state of traffic signs (e.g., flatness, inclination) from lidar data, which can be directly calculated after extracting the signs from the point cloud (Gonzalez-Jorge et al. 2013; Wen et al. 2016). However, few studies take advantage of intensity readings from mobile lidar to assess the retroreflectivity condition of the traffic signs or pavement markings.

Ai and Tsai (*2016*) propose a method for automatic sign retroreflectivity condition evaluation using mobile lidar data with a co-acquired video log. The workflow consists of four primary steps:

1. Extract the traffic sign regions of interest (ROIs) from video log images and performing segmentation based on color information in each ROI;

2. Search for the points corresponding to each cluster in a ROI from the point cloud data.

3. Correct and normalize the intensity value for each point based on distance and incidence angle.

4. Evaluate the retroreflectivity condition of the traffic sign by comparing the median value of the corrected intensity in each cluster of lidar points against a given threshold.

To obtain the reflection model of the intensity, the theoretical model from (Foley et al. 1995) is used. It is further simplified by the assumption that the fraction of the ambient lighting and the specular angle are both 0. Then, a second order function with respect to the incidence angle is applied to obtain the coefficients of the specular lighting. The empirical model parameters for a certain type of sheeting material are experimentally derived based by scanning objects at different distances and incidence angles. The retroreflectivity readings from the retroreflectometer and the calibrated intensity at the same spots on a number of traffic signs are further tested and the result shows there is a linear correlation between those readings. In the lab experiment, the impact of the repeatability of intensity value and ambient lighting condition are tested and demonstrated to be negligible for estimating retroreflectivity. This lab experiment shows another advantage of using lidar, an active sensing technique, in daytime because several studies of using the digital images to evaluate retroreflectivity of traffic signs draw two opposite conclusions on its feasibility (Khalilikhah et al. 2015; Balali et al. 2015). In the field test, the result of measuring 35 stop signs by both the retroreflectometer and mobile lidar shows that the proposed method is able to estimate the retroreflectivity using intensity with a RMSE of 3.0 $cd/m^2/lux$ on background and 4.1 $cd/m^2/lux$ on a legend.

2.5.4 Automated sign feature extraction based on intensity/intensity contrast

MLS is a useful technology for traffic sign inspection and inventory partly because it can efficiently collect a wide variety of georeferenced data simultaneously. For traffic sign detection,

recognition, and classification using MLS data, there are a number of approaches developed in the literature and in practice (Table 2.3).

Table 2.3: Characteristics Used in Traffic Sign Detection and Recognition from Mobile Lidar Data

Reference	Characteristics used in traffic sign detection and recognition					
	Color	**Intensity**	**Planarity**	**Size**	**Shape**	**Others**
Yang and Dong (2013)	-	-	√	√	√	-
Riveiro et al. (2016)	-	√	√	-	√	-
Soilan et al. (2016)	√	√	√	-	√	-
Zhou and Deng (2014)	√	√	√	√	-	Distance to the road lane
Li et al. (2016)	-	-	√	-	√	Height above the pavement
Pu et al. (2011)	√	√	√	√	√	Position, topology
Wen et al. (2016)	√	√	-	-	-	-
Vu et al. (2013)	-	√	-	-	-	Range, orientation
Wu et al. (2015)	√	√	√	-	-	Distance to the road lane
Yang et al. (2015)	-	-	√	√	-	Height above the road
Sairam et al. (2016)	-	√	-	√	-	Height above the curb
Yang et al. (2017)	-	-	√	√	-	Position

Chen et al. (2009) presents a method to detect traffic signs with a threshold of intensity and refine the results by using Random Sample and Consensus (RANSAC) and convex hull fitting. Pu et al. (2011) propose a knowledge based method of recognizing traffic signs with a detailed assumption of traffic signs in size, position, shape, orientation, color, intensity, and topological relationships. Vu et al. (2013) generate a virtual image using range and intensity from lidar data and detect planes with high intensity by applying morphological operation. The recognition of certain types of signs is then performed based on template matching. Yang and Dong (2013) propose a shape-based segmentation method, which consists of three steps: 1) labeling the point clouds into three geometric categories (linear, planar, sphere) using Support Vector Machine (SVM); 2) clustering the point clouds with different labels; 3) refining the segmentation result. Zhou and Deng (2014) propose a method for traffic sign detection and recognition based on fusion of camera and point cloud data. Position, color, intensity, and shape of the traffic sign are used for detection and supervised classification based on SVM is applied. Riveiro et al. (2016) segment the point cloud data by intensity thresholding first, then clustering the filtered point cloud, and finally recognizing different types of traffic signs by their shapes. Soilan et al. (2016)

further improve this method by considering color information in supervised classification. Li et al. (2016) extract candidate traffic signs by searching the points within a certain distance and height of the pavement based on the specifications. Then, plane fitting and the addition of geometric constraints further refine the results. There are also other methods using the height of a sign as a criterion associated with other constraints such as planarity and size (Yang et al. 2015; Sairam et al. 2016; Yang et al. 2017). Wen et al. (2016) utilize intensity values in MLS data to filter the data first and perform a sign type recognition by projecting the highly reflective points on to the camera logs. Wu et al. (2015) improve this method by considering spatial-related feature.

Because a traffic sign is usually in the shape of a plane, a plane fitting based on RANSAC (Fishler and Bolles 1980) is widely applied in traffic sign detection (Chen et al. 2009; Li et al. 2016). In addition, for checking the planarity by calculating the orientation of a plane, PCA (Jolliffe 2002) can be used for evaluating the distribution of a certain number of points (Vu et al. 2013; Yang and Dong 2013; Riveiro et al. 2016; Soilan et al. 2016). For further recognition and classification, supervised classification based on SVM (Suykens and Vandewalle 1999) is applied in some of the methods (Yang and Dong 2013; Zhou and Deng 2014; Soilan et al. 2016; Tan et al. 2016; Wen et al. 2016). In addition to the methods for mobile lidar data, there are numerous studies in intelligent driver assistance based on computer vision, which can be potentially applied in road sign detection (Mogelmose et al. 2012).

2.6 LIMITATIONS OF CURRENT LITERATURE

Several gaps and limitations were found in this review of current literature, which will be summarized in this section and guided the evaluation work in SPR-799.

For conventional retroreflectivity evaluations, the physics are being modeled or simulated in the systems with great effort; however, a key limitation is that measurements are done at few, discrete locations to be manageable. Given the high level of uncertainty and variability of the measurements themselves, we need to ask whether this modeling is necessary, or whether a technology such as mobile lidar can relatively accurately acquire that information at higher spatial resolution without following the exact geometry. Challenges associated with accurate retroreflectivity measurements on signs include inaccuracies in the geometric modeling, varying conditions during data collection, difficultly in calibration, variability in the units themselves, directionality affects, and variability in the operator skill level. Additionally, many DOTs and organizations historically have utilized approaches such as blanket replacement for signs, due to challenges in data management for information. Mobile lidar may be an option to assist with such policies of blanket replacement and may achieve cost savings for sign programs. Repeat surveys can be geospatially linked so that assets can be tracked through time. This information can ultimately be utilized for proactive management where life of assets can be predicted.

Unfortunately, there is minimal research on calibrating mobile lidar for retroreflective sign readings. Most studies in radiometric calibration are focused on a single device and focus on specific object types of interest to its application. Few DOTs have mobile lidar units and no DOTs currently have a method in place to utilize this information for radiometric calibration of their system. The radiometric calibration is highly dependent on the device itself. Hence, the relationships observed and findings of one system do not directly transfer over to another.

3.0 TESTDECK EXPIREMENTS

3.1 TEST OBJECTIVES

Three surveys were completed at the ODOT's Testdeck facility, which are described in Volume I. The research team capitalized on these tests to rigorously evaluate the capabilities of using mobile lidar to evaluate sign retroreflectivity. Three tests were completed. In the first two experiments, the mobile lidar unit was operated in a single profiler configuration where the profiler could be oriented at -60°, -30°, 0°, +30°, and +60° to the direction of travel. Only the negative orientations are capable of capturing data on the face of the sign in the direction of travel since the 0° configuration is more or less parallel to the face of the sign, capturing minimal data, and the positive orientations capture the back face of the sign. However, in the case of undivided highways, the positive orientations can capture data on the faces of the signs in the opposite direction of travel.

Related to the sign evaluation, the data from these experiments had the following objectives:

- Evaluate the coverage on the face of the sign
- Determine the quality of retroreflective readings from the sign.
- Identify if the data could be used to detect geometric abnormalities with the signs such as tilts.

These tests were not meant to be comprehensive but serve as a guide to explore the feasibility of utilizing ODOT's mobile lidar system for this purpose.

3.2 TESTDECK EXPIREMENT I

Collection of mobile lidar data from ODOT's Testdeck site (Figure 3.1) using ODOT's Pegasus: Two system with a Z+F profiler 9012 (Figure 3.1) was performed on July 28, 2016 starting at 8am. The Testdeck is located on the westbound right travel lane of Highway OR-22 between mileposts 12.25 and 12.5 (44.825663 N, 122.813566 W), outside of Salem and near Stayton.

For this first evaluation, the project team obtained mobile lidar data using different truck speeds and sensor orientations using ODOT's Leica Pegasus: Two (Figure 3.1). (Note that for this test, ODOT was only operating with a single profiler solution on the mobile lidar unit). Data at each speed was collected twice: one with the sensor rotation of 0° and another one with -30°. At that time, ODOT normally operated the MLS system in 0° orientation, which provides profiles along the roadway perpendicular to the travel direction. However, the -30° orientation provides the ability to capture information on the front face of street signs in both directions in a single pass. Table 3.1 shows the scanning settings for each pass of the lidar data collection.

Figure 3.1: ODOT's mobile lidar system collecting data on the Testdeck.

Table 3.1: Test Configurations and Schedule for Testdeck I.

Pass #	Start Time	Speed (mph)	Profiler unit rotation (°)	Traffic control required	Approximate time (mins)
0	8:00	N/A	Meet at site, onsite safety briefing, review MLS procedure, and perform MLS initial site calibration process	N	40
1	8:10	45	0 (normal orientation)	N	10
2	8:20	55	0 (normal orientation)	N	10
3	8:30	55	-30	N	10 + rotate scanner
4	8:40	45	-30	N	10
5	8:50	35	-30	Y	10 + placing traffic control
6	9:00	25	-30	Y	10
7	9:10	35	0 (normal orientation)	Y	10 + rotate scanner
8	9:20	25	0 (normal orientation)	Y	10
9*	9:30	25	0 (normal orientation)	Y	10

**Pass 9 was a repeat pass since the data were not recorded on Pass 8 due to a blunder.*

Considering the rotation speed of the Z+F profiler on the Pegasus system (200 revolutions per second), transverse orientation of the test stripes, and the width of pavement stripes, the project team collected data with lower truck speeds in order to obtain enough sample points on each stripe. (Note that the speeds were be insufficient for detailed coverage at the 0° orientation for the transverse stripes; however, the -30° orientation provides adequate coverage on the transverse stripes). In order to evaluate data quality captured on longitude stripes in faster speeds, the project team also collected data with speeds of 45 and 55 mph; however, they have limited coverage on the transverse striping with the 0° orientation (Table 3.2).

Table 3.2: Calculated Profile Spacing for Several Vehicle Speeds With MLS Configured in the 0° Orientation.

Speed (mph)	Speed (m/s)	Profile Spacing (m)	#Profiles per stripe
5	2.2	0.011	13.6
10	4.5	0.022	6.8
15	6.7	0.034	4.5
20	8.9	0.045	3.4
25	11.2	0.056	2.7
30	13.4	0.067	2.3
35	15.6	0.078	1.9
40	17.9	0.089	1.7
45	20.1	0.101	1.5
50	22.4	0.112	1.4
55	24.6	0.123	1.2

The order of data collection passes was designed for efficiency. The project team started with high-speed passes in the morning (approximately 9 am) to keep up with traffic. Once the high speed data collections were completed, the project team ran low-speed paths which required blocking the lane with signs and cones for traffic control. While these lower speeds were primarily related to improving point density on the pavement markings being evaluated in the test, they also provided higher resolution scans of the signs improving the statistical robustness of the evaluation. Each pass took approximately 10-15 minutes to complete, including the time required for turning around. Only a few minutes were required to switch the sensor rotation from 0° to -30°.

In between each pass, the vehicle turned around at Exit 12. Scanning was continued to capture the data from the Eastbound return travel as well (at 55 mph each time) in an effort to provide additional data to support the analysis, even though it was collected on the opposite side of the road. Ultimately, it was found that the view of the Testdeck was too limited from these passes for the analysis.

After completion of the passes, the MLS team downloaded and commenced processing the MLS data. The project team archived a copy of all source files (GPS, IMU, scanner data streams) from the collection as well as the processed (georeferenced) scans in ASPRS LAS 1.2 format that were later provided by ODOT.

3.3 TESTDECK EXPIREMENT II

For the lidar data acquisition in this second experiment (Table 3.3), the project team collected data on the Testdeck using the mobile lidar system (Leica Pegasus:Two) with ODOT on both traffic lanes and the shoulder in different orientation settings (-60°, -30°, 0°, 30°, and 60°). In this way the project team covered the entire area of interest with different view angles for testing the radiometric calibration methods. For running mobile lidar on the left lane, the project team collected data at a slower but safe speed using hazard lights. After two passes on the left lane with -30°, and +30° orientation setting, the traffic control was setup to block the right lane where the Testdeck is located. Then the project team kept the Testdeck and the shoulder clear to run the two passes on the shoulder with the -30°, and 30° orientation setting at a speed of 25 mph. Next, five passes on the right lane with -60°, -30°, 0°, +30°, +60° orientation with a speed of 25 mph were performed. After confirming all 9 passes were collected properly, a copy of the raw data was downloaded to a USB drive provided by OSU and another copy taken to Oregon DOT for subsequent processing (geo-referencing).

Table 3.3: Summary of Data Collection for Mobile Lidar System at Testdeck I

Pass #	Lane	Orientation (°)	Speed (mph)
1	Left	+30	25
2	Left	-30	25
3	Right Shoulder	+30	25
4	Right Shoulder	-30	25
5*	Right	+60	25
6	Right	+30	25
7	Right	0	25
8	Right	-30	25
9	Right	-60	25

**Note that that a system exception occurred during the first pass on the right lane. It was resolved by restarting the system, creating a new mission and reinitializing the system and the pass was repeated.*

3.4 TESTDECK EXPIREMENT III

Testdeck III was completed on July 25, 2017 with the same considerations as Testdeck II. However, between Testdeck II and Testdeck III, ODOT Geometronics updated the system with a second profiler which locked the sensor orientation into -30°/+60°.

For the lidar data acquisition in this test (Table 3.4), the project team collected data on the Testdeck using the mobile lidar system (Leica Pegasus:Two) with ODOT on both traffic lanes and the shoulder in the fixed orientation (-30°/+60°). In this manner, the project team can cover the entire area of interest with different view angle for testing the radiometric calibration methods. For the three passes of running mobile lidar on the left lane, the data were collected in a speed of 25, 35, and 45 mph respectively. The passes on the left lane were performed with a rolling slowdown to avoid the cones blocking the laser beams and creating shadows in the data. After three passes on the left lane, the traffic control was performed to block the right lane where

the Testdeck is located. The shoulder was kept clear to run the two passes at speeds of 15 and 25 mph respectively. Next, five passes on the right lane with a speed of 15, 25, 35, 45, and 55 mph were performed. After confirming all the 9 passes were collected properly, a copy of the raw data was downloaded to the USB drive provided by OSU and another copy taken to Oregon DOT for processing.

Table 3.4: Summary of Data Collection for Mobile Lidar System at Testdeck II

Pass #	Lane	Orientation (°)	Speed (mph)
1	Left	-30/+60	25
2	Left	-30/+60	35
3	Left	-30/+60	45
4	Shoulder	-30/+60	15
5	Shoulder	-30/+60	25
6	Right	-30/+60	15
7	Right	-30/+60	25
8	Right	-30/+60	35
9	Right	-30/+60	45
10	Right	-30/+60	55

3.4.1 TLS

To capture the detailed information on the Testdeck for further analysis, the project team collected the data using a Leica P40 on the Testdeck. The scan positions were set up every 20 meters to cover the Testdeck while a GPS receiver on top of the scanner collected Oregon Real-Time GNSS Network (ORGN) data during the scan. The scans started from the west ends of the Testdeck, and 12 scans were acquired with the scan settings listed as follows:

- Field of view: Horizontal: Target All = 0° - 360°, Vertical: -55 – 0°
- Scanning Resolution: 0.01m @ 30m
- Mode: Range, Sensitivity: Normal
- Imaging: Resolution: 1920 x 1920, HDR: No

3.5 TEST LIMITATIONS

During the course of this research, ODOT upgraded their mobile lidar system to support a dual-profiler configuration (-30°/+60°) which can improve the data quality (*e.g.*, point density). However, this configuration no longer allows the flexibility of switching to the other configurations (e.g., 0° and +60°) as was conducted on the previous tests. Hence, the data acquisition strategy varied from Testdeck II.

3.6 TEST RESULTS

Based on the results of Testdeck I and II, it was determined that the Leica Pegasus:Two system typically saturates on retroreflective signs (Figure 3.2). This creates two problems for obtaining sign condition information. First, because the received signal amplitude exceeds the thresholds of the system, intensity values are truncated (saturated) and cannot be calibrated or used in estimating retroreflectivity. Second, the saturated intensity values lead to errors in the range calculation, resulting in incorrect coordinates for the sign. The latter effect results from the well-known lidar "range walk" phenomenon (*Brock et al. 2002; Hug et al. 2004; Shrestha et al. 2007*), in which the detected range is dependent on the received signal amplitude. Although lidar data can be corrected to remove the effects of range walk, in the case of fully saturated intensities, range walk correction may not be possible, leading to incorrect coordinates.

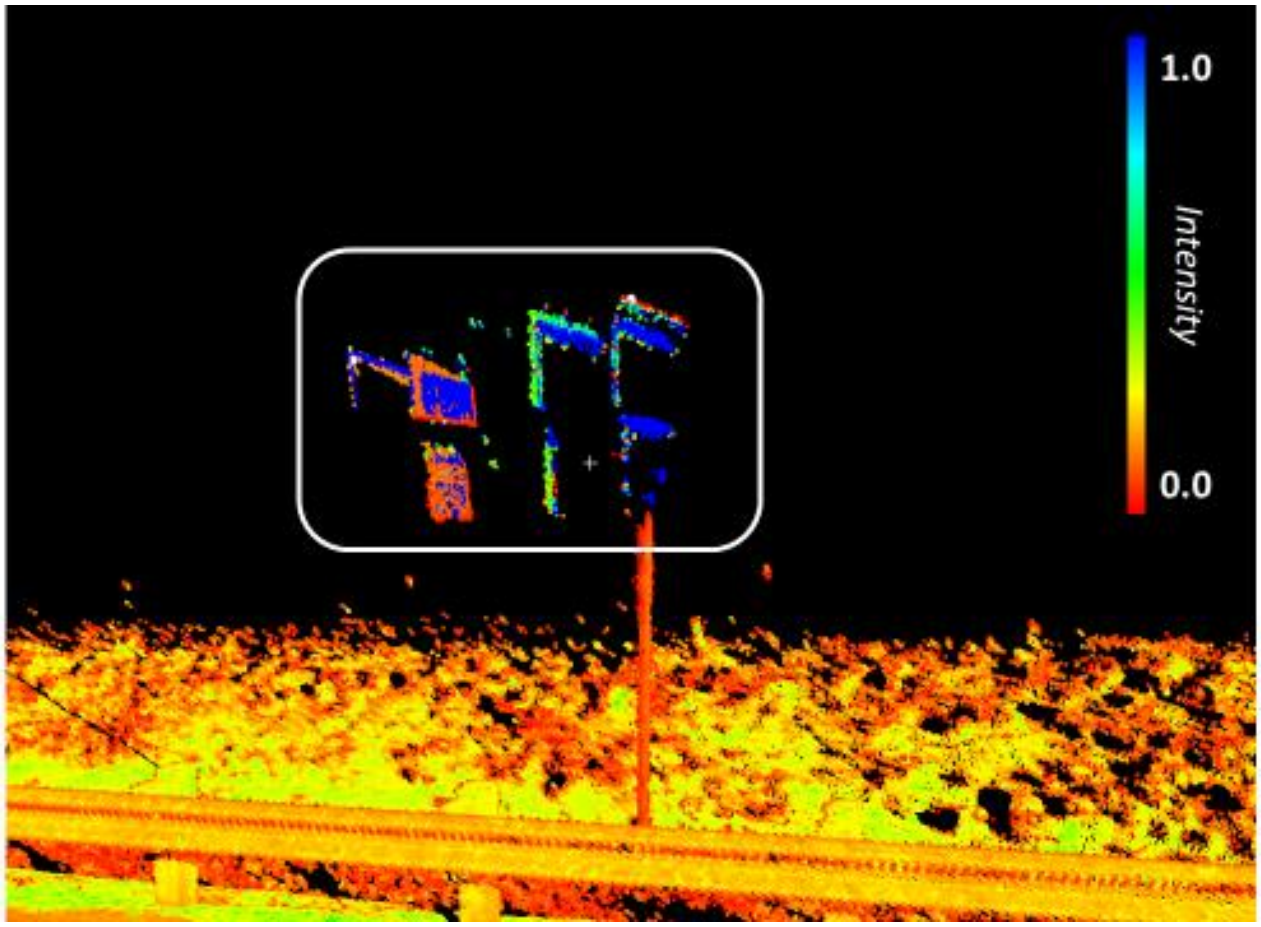

Figure 3.2: Saturation (blue points) and Range Walk effects observed in the Testdeck dataset

Another limitation observed in the data is that color information assigned to the point cloud may not be from the imagery acquired from the same side of a sign captured by the scanner. The research team investigated multiple datasets and found that it is not consistent under what condition this artifact occurs (Figure 3.3).

Some TLS work are better suited for sign evaluation than others based on their wavelength, emittance power, and receiving optics. One advantage TLS has over mobile lidar is the wider

range of values in range and angle of incidence typically obtained (Figure 3.4). Radiometric calibration of ODOT's TLS units could be further explored in future research, if desired. However, TLS would likely only be economically feasible to employ at locations such as major urban intersections where the spatial density of signs is high.

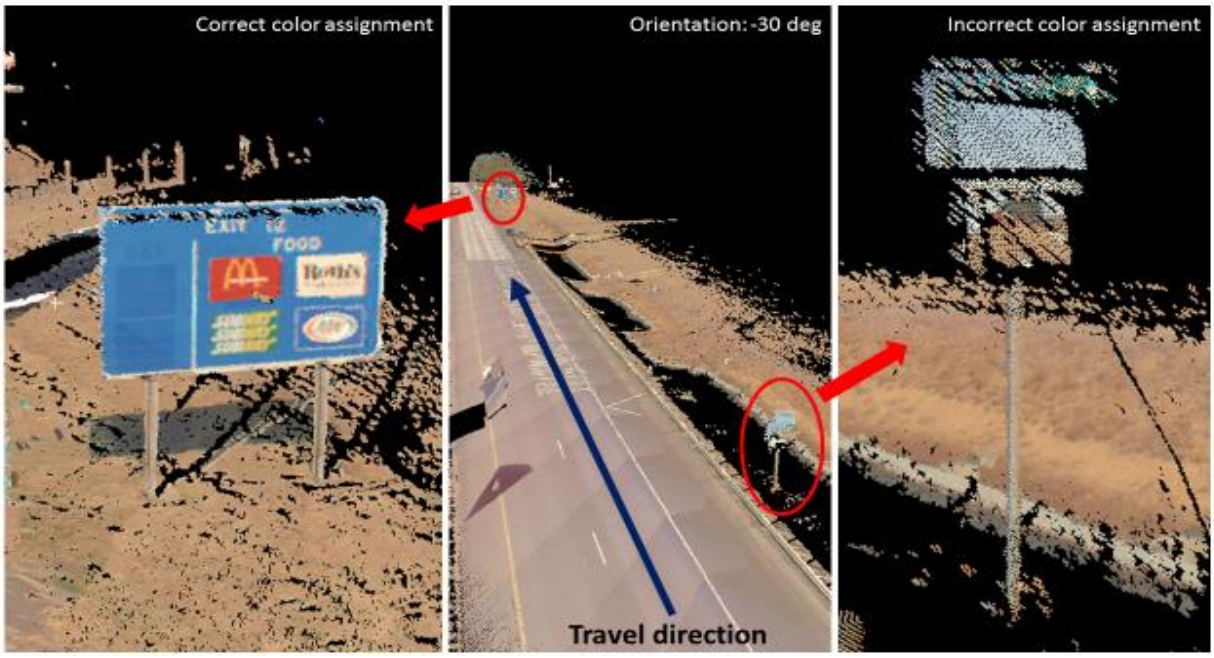

Figure 3.3: Assignment of the color from the reverse side of a sign (Testdeck)

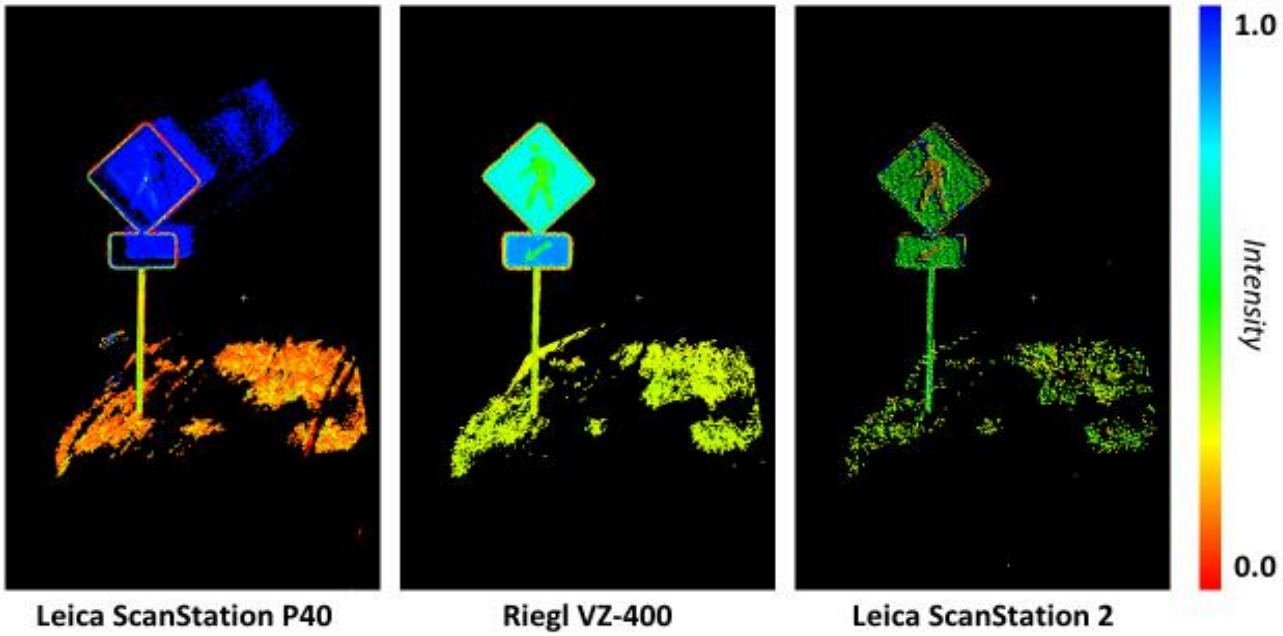

Figure 3.4: Performance of different terrestrial laser scanners on capturing signs from the wet/dry test documented in Volume I.

4.0 SIGN EVALUATION

4.1 TEST OBJECTIVES

As noted above, the overarching objective of the research described in Volume II (this volume) was to investigate whether the procedures developed for pavement marking retroreflectivity evaluation using mobile lidar could also be extended to sign retroreflectivity evaluations. Based on the results of the Testdeck experiments, it was determined that the Leica Pegasus:Two system typically saturates on retroreflective signs. Hence, in this experiment, the project team performed additional testing on the utility of mobile lidar for sign evaluation to see if some corrections were possible. The test consisted of the following steps:

1. Coordinated with ODOT's sign shop (Meghan Jorgenson, POC) to set aside as many different sign types and conditions, colors as available. The test was designed to use several signs below the retroreflectivity limit to see if those still saturate with the mobile lidar system.

2. Set up signs in an ODOT Maintenance Yard.

3. Measured sign retroreflectivity with a handheld reflectometer (Road Vista 922).

4. Performed several runs with the mobile lidar signs. Additionally, the project team will vary the scanning geometry (e.g., -30˚, -60˚).

The analysis included assessing the capability to correct for range walk, followed by geometric condition assessment. The ultimate goal of this test was to document both the capabilities and limitations of mobile lidar for sign condition assessment.

4.2 TEST DESCRIPTION

The signs test (Figure 4.1 to Figure 4.4) was coordinated with the ODOT Sign Shop, including Steve Barner, ODOT Sign Crew, Meghan Jorgenson, Supply Operations Manager, ODOT Office of Maintenance and Operations and Shawn McKnight, ODOT Sign Shop. The data acquisition for the signs test was completed on June 19, 2017. A number of signs were set up signs in an ODOT Maintenance Yard and 12 passes of ODOT Geometronics' Leica Pegasus:Two were completed (Figure 4.4).

Figure 4.1: Mounting signs in ODOT's Maintenance Yard.

Figure 4.2: Additional signs (top) and data collection with ODOT's Pegasus:Two (bottom).

Figure 4.3: Mobile lidar truck with Leica Pegasus: Two and tripod-mounted Leica ScanStation P40 in the foreground.

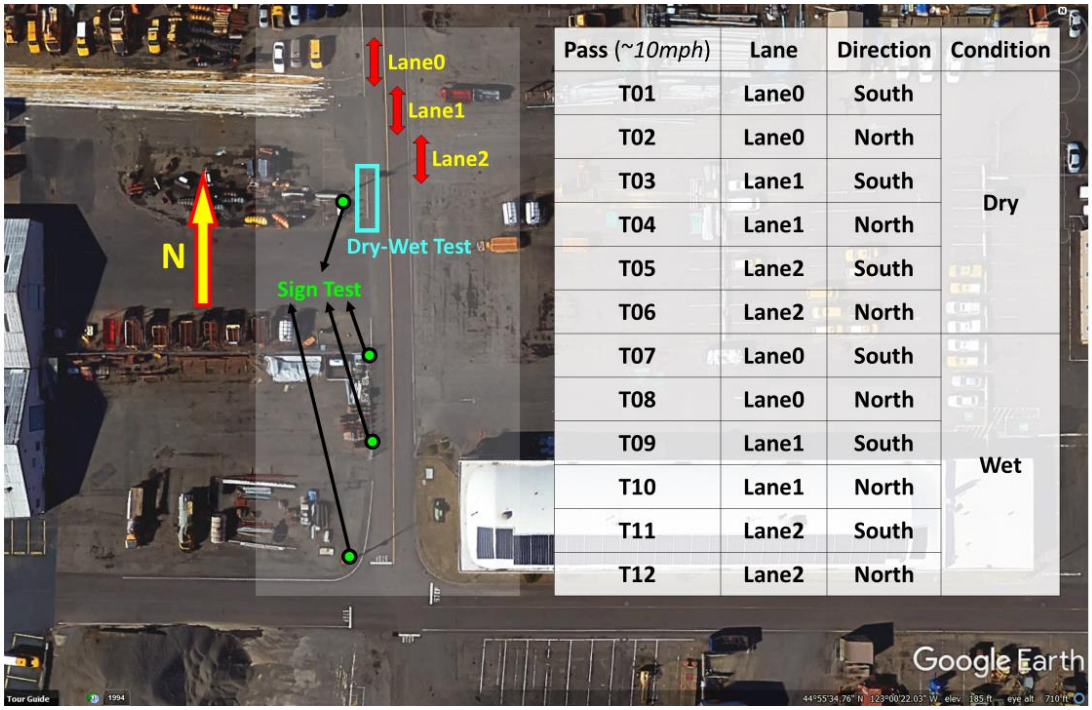

Pass (~10mph)	Lane	Direction	Condition
T01	Lane0	South	Dry
T02	Lane0	North	
T03	Lane1	South	
T04	Lane1	North	
T05	Lane2	South	
T06	Lane2	North	
T07	Lane0	South	Wet
T08	Lane0	North	
T09	Lane1	South	
T10	Lane1	North	
T11	Lane2	South	
T12	Lane2	North	

Figure 4.4: Signs test layout and list of mobile lidar passes.

4.3 TEST RESULTS AND ANALYSIS

Among the signs provided by the Sign Shop, a “SCHOOL BUS STOP AHEAD” sign (Figure 4.6) was first selected for analysis, because it contained some cracks, yet, from visual inspection,

was anticipated to still maintain its retroreflectivity. In the point cloud data, all the passes capture this sign, with most of the points on the sheeting being saturated (Figure 4.66).

Figure 4.5: "SCHOOL BUS STOP AHEAD" sign and the resulting mobile lidar data from six passes of the Lieca Pegasus:Two.

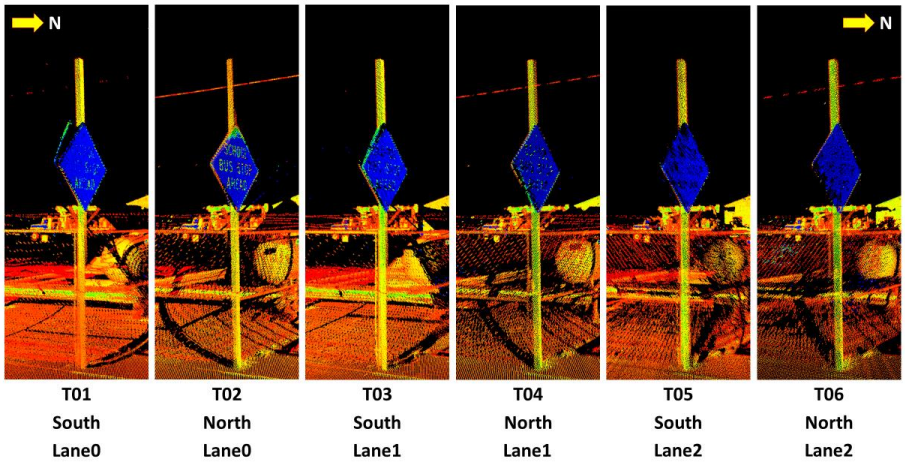

Figure 4.6: Blue colors indicate saturation (i.e., intensity values at or beyond the upper limit of the lidar system's measurable range).

Since the saturation of the mobile lidar data on signs--even those in poor condition--severely limits the ability to evaluate retroreflectivity (or to make use of the intensity data in any meaningful way), the project team next selected a number of significantly worn signs to investigate whether the intensity values could help detect failing signs. Two particular signs were selected: 1) a "SLOW" sign, which was worn and had several bullet holes on it, and 2) a "STOP" sign, worn significantly to the extent that the "P" character was scarcely recognizable (Figure 4). In some passes, the lidar intensity data from these signs contained valid values (i.e., below the

saturation threshold) in some areas on the sign, as opposed to being saturated across the entire sign. However, all the points on the stop sign from the pass T1, T4, and T6 were saturated, while in the other passes, even though not all the points are saturated, the apparent worn part of the sign (right to the character "P") is still saturated. For the "SLOW" sign, the points on it from T1, T2, T3, and T4 are saturated, while the other passes contain some unsaturated points. The overall finding from this test is that, even with clearly failing signs, the mobile lidar intensity data are too frequently saturated to be of use.

(a)

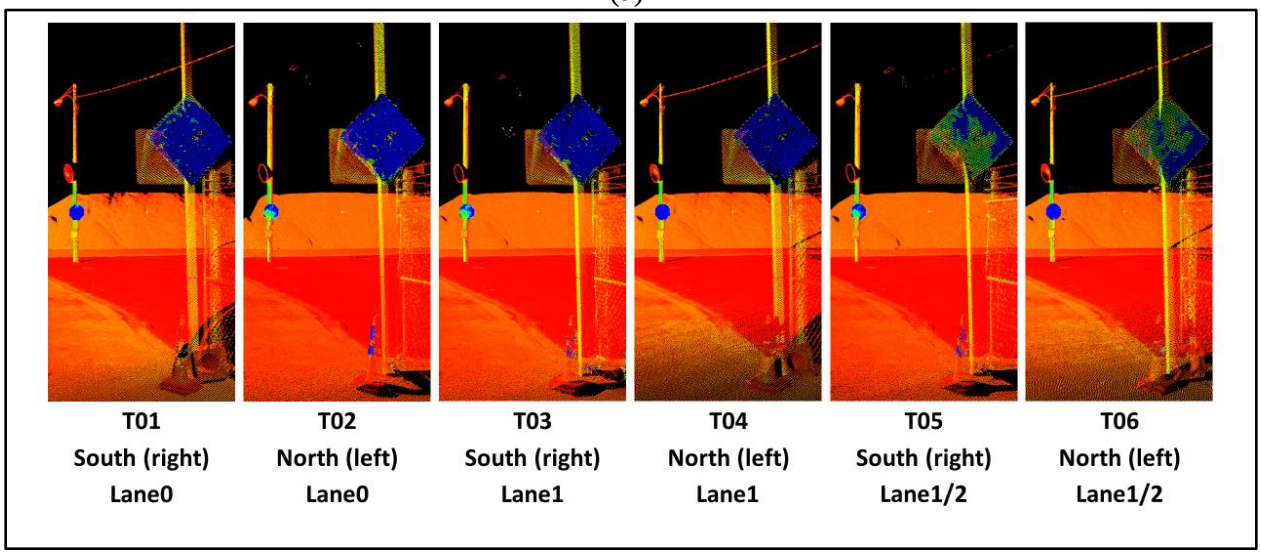

(b)

Figure 4.7: (a) Photographs showing the damaged signs utilized in the test and (b) example point clouds obtained on the signs of interest. Blue indicates saturation of intensity.

As the final step in this test, the project team analyzed the mobile lidar data of "TEST" signs that ODOT uses to train and calibrate for visual evaluation (Figure 4.8 a). Unfortunately, once again, the mobile lidar data for the "TEST" signs were saturated in all passes in nearly all areas of each sign (Figure 4.8 b). Additionally, significant range walk was observed on the green "TEST" sign, although, interestingly, not on the red "TEST" sign above it.

(a)

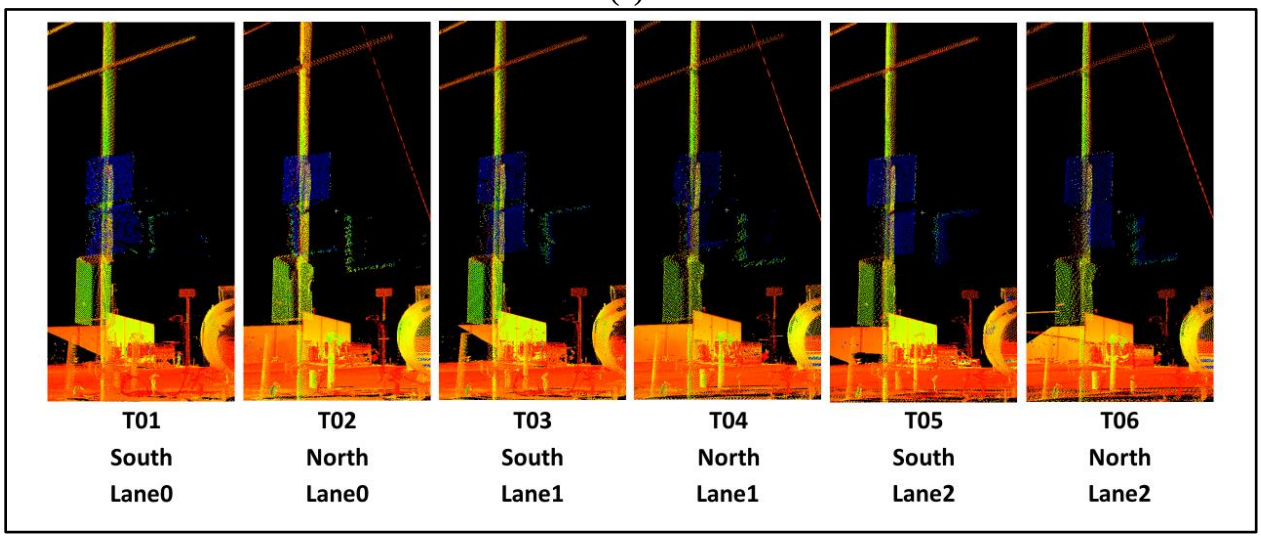

(b)

Figure 4.8: "TEST" signs used by ODOT to train and calibrate visual inspectors.

Because of the inconsistency of the intensity on signs from different passes, as well as the frequent range walk effect, the overall findings of this test were that: 1) mobile lidar systems are

very sensitive to the scan geometry to a retroreflective traffic sign, 2) the data generally fail to represent the condition of a sign in terms of providing results comparable to those obtained via visual evaluation. Therefore, in this case, the project team concluded that the mobile lidar data is currently of limited use in ODOT's evaluation of the retroreflectivity of traffic signs.

4.4 TEST LIMITATIONS

It would have been possible to conduct additional tests of signs, using the mobile lidar system to scan a wider range of types, colors and conditions of signs. However, the results of the tests described above were deemed sufficient to conclude that, at the present time, the mobile lidar intensity data is of relatively little value for evaluation of sign retrorefelctivity, due to the issues of saturation and range walk. This is in sharp contrast to the mobile lidar system's usefulness for pavement marking retroreflectivity assessment, as described in detail in the Volume I report. In theory, it should be possible to modify the lidar system to prevent intensity saturation on signs (e.g., using a neutral density filter in the lidar receiver). However, such modifications could severely limit the lidar system's performance (especially, its maximum range) and could also introduce unexpected artifacts. A better approach would be to work collaboratively with the lidar system manufacturer on future enhancements that would increase the dynamic range of the system and prevent saturation from retroreflective signs, and this is a recommended topic for follow-on research. However, it must be noted that such modifications would affect the radiometric calibration results developed in Volume I.

5.0 CONCLUSIONS AND RECOMMENDATIONS

Volume II explored the feasibility of utilizing ODOT's mobile lidar unit for sign retroreflectivity and condition evaluation. The key reasons mobile lidar was effective for pavement marking evaluation (Volume I) and not for signs include:

1. Saturation of the lidar data points from retro-reflective signs caused 'ghost' images (aka range walk). In pavement markings, a larger range of density was witnessed with highly reflective lidar returns versus worn (and not so reflective) imagery. Signs, however, tend to be more evenly worn compared to pavement markings. Additionally, sign retroreflectivity standards require higher levels of retroreflectivity in comparison to those being considered for pavement markings.

2. When readings on signs from mobile lidar are collected at low angles of incidence, the sampling on the sign is affected due to the obliquity. In contrast, configurations resulting in high angles of incidence result in better sampling on the sign face; however, this also can contribute to the saturation from higher return signal strength. Nevertheless, because the sign sheetings are designed to be omnidirectional in retroreflectivty, saturation occurs from too much energy being returned to the scanner in both the -30° and -60° configurations on the signs facing the direction of travel. (Similar results were observed for signs in the opposite direction of travel in the +30° and +60° orientations). In contrast, pavement markings on the road surface (discussed in Volume I) are observed at more oblique angles to the scanner, returning less energy and leading to fewer problems with saturation.

This research evaluated the capabilities of ODOT's mobile laser scanner to perform retroreflectivity analysis on signs. The following conclusions can be drawn:

- The mobile lidar unit was **not** successful in evaluating the retroreflectivity of signs. Across a wide range of geometric conditions, the lidar intensity values were saturated even on signs with low retroreflectivity.

- Laser intensity (and subsequently retroreflectivity) values saturate on sign faces leading to positional inaccuracies (i.e., range walk) up to several meters, as well as unreliable intensity measurements (even for signs at the failing point for retroreflectivity for signs). These positional inaccuracies may not be suitable for surveying for design applications, but could be satisfactory for asset management applications. In particular, the post of the sign is not significantly affected by range walk effects and provides an accurate location for the sign for a base map.

- Other systems studied in the literature review (e.g., *Ai et al. 2016*) have been shown to provide acceptable results for sign retroreflectivity, but unfortunately, ODOT's current system cannot be used for this purpose in its current configuration.

- Data density on the sign face is heavily dependent on sensor configuration. For example, -60° is optimal compared to 0°, which results in very sparse data, if any. The +30° and +60° configurations do capture the rear of the sign rather than the face; however, they can be used to capture signs for the lanes in the opposite direction of travel. Regardless, these other configurations are no longer options in the dual configuration of ODOT's current mobile lidar system with dual profilers, which is locked in with sensors oriented at -30° and 60°.

- With sufficient density, contrasting text and symbols can be read on the signs when viewing the point cloud colored by intensity.

- Another limitation observed in the data is that there is a chance that the camera orientation captures imagery from the reverse of the sign rather than in the direction of travel. As a consequence, some automatic sign detection approaches taking advantage of computer vision techniques, and potential retroreflectivity evaluation based on daytime imagery (Balali et al. 2015) are not applicable in this case.

- From preliminary investigation, the TLS appeared to work better for sign evaluation given the differences in range and angle of incidence possible with TLS. Radiometric calibration of ODOT's TLS units could be further explored in future research, if desired. However, TLS would likely only be economically feasible to employ it at locations such as major urban intersections where the spatial density of signs is high but would not be feasible on long highway sections unless utilized in a stop and go fashion.

5.1 ADDITIONAL CONSIDERATIONS

In developing the work plan for SPR-799 prior to starting the project, the research team considered the possibility that solar illumination (in particular, the sun's altitude and azimuth, as well as cloud conditions) could adversely affect the ability to reliably estimate retroreflectivity from the calibrated lidar intensity data. However, our findings from the literature review and preliminary analysis of possible testing procedures revealed that the effects of solar illumination can generally be considered negligible. While solar illumination can increase noise in lidar measurements, and the sun position can impact intensities in laser scanning data (e.g., *Dassot et al. 2011*), specific sun-scanner-surface geometries would be required for solar illumination to significantly impact the calibrated lidar intensity data in this work. Due to the low probabilities of occurrence of these specific geometries, and the ability to detect and eliminate the problematic data if they were to occur, it was determined that this effect did not merit inclusion in the project plan. Nevertheless, signs would be more sensitive to these effects than pavement markings, and, if the evaluation of retroreflectivity of signs from mobile lidar is extended in follow-on research, the potential impacts of solar illumination could be reassessed.

5.2 FINAL REMARKS

While ODOT's current system is not capable of performing sign retro-reflectivity evaluations in all its currently possible configurations, there are other possibilities that ODOT can consider.

For example, other systems studied in the literature review (e.g., *Ai et al. 2016*) have been shown to provide acceptable results for sign retroreflectivity. For example, Figure 5.1 shows an example of a point cloud collected with a different mobile lidar system that utilizes Riegl V-line scanners by MNG surveys at the ODOT mobile lidar test course in Salem. In this case, the points acquired on the sign are still saturated; however, they do not experience range walk. In this case, the manufacturer has tuned their scanner to be able to read a wider range of intensity values to improve detection of reflective targets at the expense of decreased resolution of intensity values on other objects of lower retroreflectivity. Hence, it is unclear if that system will perform as well on pavement markings, which are of lower retro-reflectivity. They also implement look-up-table correctors to minimize range walk.

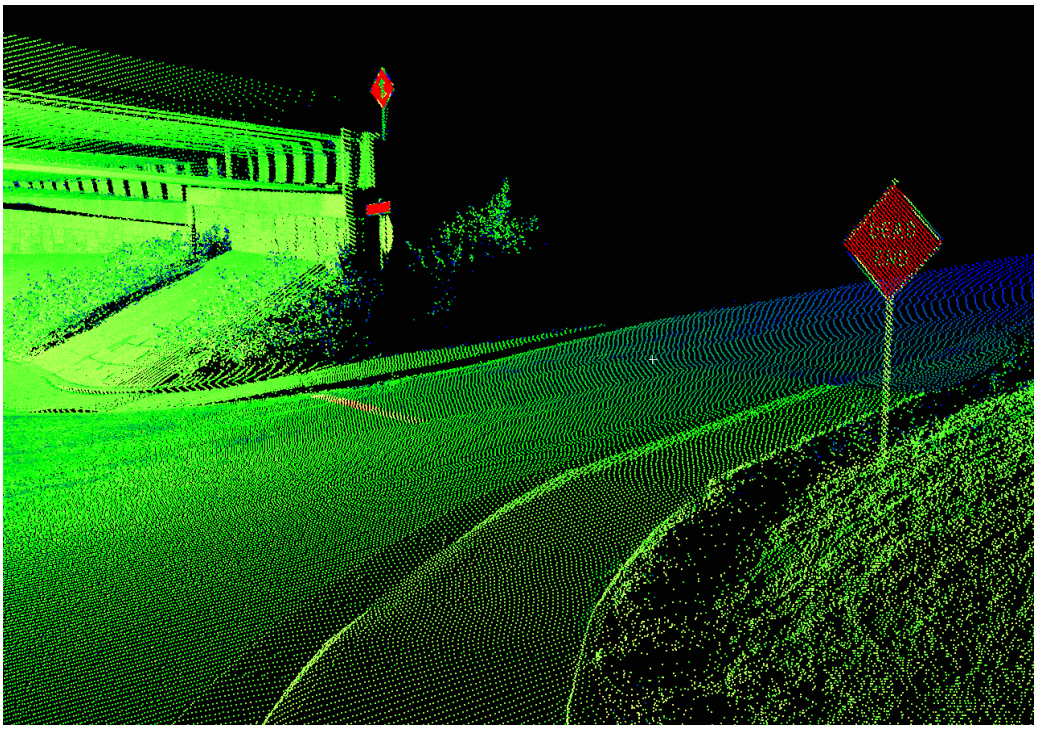

Figure 5.1: Example point cloud with less saturation on signs collected at the ODOT mobile lidar test course in Salem, OR by MNG surveys using a different scanner. (Data Courtesy of McMullen-Nolan (MNG) Surveys)

To continue to explore the possibility of utilizing retro-reflectivity evaluation with mobile lidar, the following actions are recommended:

- In the near future, ODOT should communicate their interest in using mobile lidar for sign retroreflectivity analysis to the current manufacturer (Leica Geosystems) so that the manufacturer can consider utilizing a different scanner on future mobile lidar configurations or tuning the scanner's dynamic range. It is likely the manufacturer can develop a potential configuration in a future upgrade of the system. They may also be able to develop look-up-table correctors to minimize range walk with the current system.

- When ODOT is in the process of purchasing a new mobile lidar system at the appropriate time in the future, the potential for sign retroreflectivity evaluation should be considered in the decision making amongst other factors of how the system is being utilized. Note that there are many other factors and purposes that should be considered besides signs including the radiometric calibration and associated tools for the pavement markings described in Volume I as well as other initiatives in place at ODOT.

- Prior to utilizing a new mobile lidar system for this purpose, research verifying its capabilities and limitations and develop the appropriate radiometric calibration, automated sign extraction algorithms, and analysis tools (similar to those developed for pavement markings) should be implemented.

Specialized optical attenuation filters can be applied to the receiving or emitting optics of the system to potentially obtain retroreflectivity measurements on the signs; however, such approaches will likely result in substantial loss of information on dark (e.g., pavement) or wet surfaces where the signal strength is low. Furthermore, such hardware modifications would invalidate the radiometric calibration produced for the pavement markings in this research. They would likely degrade other data collected from the system, reducing the benefit of being able to collect data for a wide range of purposes from one platform. Hence, this type of modification is not recommended at this time.

6.0 REFERENCES

Ahokas, E., Kaasalainen, S., Hyyppä, J. & Suomalainen, J. (2006). Calibration of the Optech ALTM 3100 laser scanner intensity data using brightness targets. *International Archives of Photogrammetry, Remote Sensing and Spatial Information Sciences, 36,* 14-20.

Ai, C. & Tsai, Y.J., (2016). An automated sign retroreflectivity condition evaluation methodology using mobile LIDAR and computer vision. *Transportation Research Part C: Emerging Technologies, 63,* 96-113.

American Association of State Highway and Transportation Officials (2015). *Standard Specification for RetroReflective Sheeting for Flat and Vertical Traffic Control Applications* (AASHTO M268-15).

American Society for Testing and Materials. (2016). *Standard Specification for Retroreflective Sheeting for Traffic Control* (ASTM D4956-16b). Retrieved from https://doi.org/10.1520/D4956-16B

American Society for Testing and Materials. (2009). *Standard Test Method for Measurement of Retroreflective Signs Using a Portable Retroreflectometer at a 0.2 Degree Observation Angle* (ASTM E1709-09). Retrieved from https://doi.org/10.1520/E1709-09

Austin, R.L., & Schultz, R.J. (2009). *Guide To Retroreflection Safety Principles And Retrorereflective Measurements* (Rep.). San Diego, CA: RoadVista. Retrieved from https://www.gamma-sci.com/wp-content/uploads/2012/06/Retroreflectivity-Guide-RoadVista.pdf

Balali, V., Sadeghi, M.A. & Golparvar-Fard, M., (2015). Image-based retroreflectivity measurement of traffic signs in day time. *Advanced Engineering Informatics, 29*(4), 1028-1040.

Baltsavias, E.P., 1999. Airborne laser scanning: basic relations and formulas. *ISPRS Journal of Photogrammetry and Remote Sensing, 54,* 199-214.

Briese, C., M., Pfennigbauer, H., Lehner, A., Ullrich, A., Wagner, W., & Pfeifer, N., (2012). Radiometric Calibration of Multi-Wavelength Airborne Laser Scanning Data. *ISPRS Annals of the Photogrammetry, Remote Sensing and Spatial Information Sciences (ISPRS Annals) 7,* 335–340.

Brock, J.C., C.W. Wright, A.H. Sallenger, W.B. Krabill, and R.N. Swift, (2002). Basis and methods of NASA airborne topographic mapper lidar surveys for coastal studies. *Journal of Coastal Research,* 18(1), 1-13.

Burns, D., Hedblom, T., & Miller, T. (2008). Modern Pavement Marking Systems: Relationship Between Optics and Nighttime Visibility. *Transportation Research Record: Journal of the Transportation Research Board*, 2056, 43-51.

Carlson, P.J., Miles, J.D., Pike, A.M., & Park, E.S. (2007). *Evaluation of Wet-Weather and Contrast Pavement Marking Applications: Final Report* (Report Number 0-5008-2). Texas Transportation Institute.

Carlson, P.J. & Hawkins Jr, H.G., (2003). *Updated minimum retroreflectivity levels for traffic signs* (FHWA-RD-03-081). U.S. Department of Transportation, Federal Highway Administration.

Carlson. P.J., Hawkins Jr, H.G., Schertz, G.F., Mace, D.J., & Opiela, K.S. (2003). Developing updated minimum in-service retroreflectivity levels for traffic signs. *Transportation Research Record: Journal of the Transportation Research Board*, *1824*, 133-43.

Chen, X., Kohlmeyer, B., Stroila, M., Alwar, N., Wang, R. & Bach, J. (2009). Next generation map making: geo-referenced ground-level LIDAR point clouds for automatic retroreflective road feature extraction. *Proceedings of the 17th ACM SIGSPATIAL International Conference on Advances in Geographic Information Systems*, 488-491.

Dassot, M., T. Constant, and M. Fournier, (2011). The use of terrestrial LiDAR technology in forest science: application fields, benefits and challenges. *Annals of Forest Science*, 68(5), 959-974.

Federal Highway Administration, FHWA, (2009). Sign Retroreflectivity Guidebook: How to Meet the New National Standard: U.S. Department of Transportation. Retrieved from https://d2dtl5nnlpfr0r.cloudfront.net/tti.tamu.edu/documents/FHWA-CFLTD-09-005.pdf.

Federal Highway Administration (FHWA), 2012. Manual for Uniform Traffic Control Devices 2009 Rev2. U.S. Department of Transportation. Retrieved from https://mutcd.fhwa.dot.gov/

Gonzalez-Jorge, H., Riveiro, B., Armesto, J. & Arias, P., (2013). Evaluation of road signs using radiometric and geometric data from terrestrial LiDAR. *Optica Applicata*, *43*(3), 421-433.

Hawkins, N.R., Pike, A.M., Smadi, O.G., Knickerbocker, S. and Carlson, P.J., 2015. *Evaluating All-Weather Pavement Markings in Illinois: Volume 1*. Illinois Center for Transportation/Illinois Department of Transportation.

Höfle, B. & Pfeifer, N. (2007). Correction of laser scanning intensity data: Data and model-driven approaches. *ISPRS Journal of Photogrammetry and Remote Sensing*, *62*(6), 415-433.

Hug, C., A. Ullrich, & A. Grimm, (2004). Litemapper-5600-a waveform-digitizing LiDAR terrain and vegetation mapping system. *International Archives of Photogrammetry, Remote Sensing and Spatial Information Sciences*, *36*(8), W2.

Jelalian, A.V. (1992). *Laser radar systems*. Norwood, Massachusetts, Artech House 292 pp.

Jensen, J.R. (2005). *Introductory digital image processing: a remote sensing perspective*, 3rd Ed., Pearson, Prentice Hall, Upper Saddle River, New Jersey, 526 pp.

Jolliffe, I., (2002). *Principal component analysis*. John Wiley & Sons, Ltd., Hoboken, New Jersey.

Jutzi, B., & Gross, H. (2009). *Normalization of Lidar Intensity Data Based On Range and Surface Incidence Angle*. (Bretar, F. et al.: Laserscanning '09: ISPRS Workshop. 1.-2. September 2009 Paris, France. (International archives of photogrammetry, remote sensing and spatial information sciences 38 Part 3 / W8).)

Kaasalainen, S.A., Jaakkola, M. Kaasalainen, A., Krooks, A., & Kukko, A. (2011). Analysis of incidence angle and distance effects on terrestrial laser scanner intensity: search for correction methods. *Remote Sensing*, *3*(10), 2207-2221.

Kaasalainen, S.A., Krooks, A., Kukko, & Kaartinen, H. (2009). Radiometric calibration of terrestrial laser scanners with external reference targets. *Remote Sensing*, *1*, 144–158.

Kashani, A.G., Olsen, M.J., Parrish, C.E., & Wilson, N. (2015). A Review of Lidar Radiometric Processing: from ad hoc Intensity Correction to Rigorous Radiometric Calibration. *Sensors*, 15, 28099-28128; doi:10.3390/s151128099.

Khalilikhah, M., Heaslip, K. & Song, Z., (2015). Can daytime digital imaging be used for traffic sign retroreflectivity compliance? *Measurement*, *75*, 147-160.

Kirk, A.R., Hunt, E.A., & Brooks, E.W. (2001). *Factors Affecting Sign Retroreflectivity: Final Report* (SR 514). Oregon Department of Transportation Research Group. Retrieved from: https://ntl.bts.gov/lib/10000/10500/10531/FASR.pdf

Kopf, J. (2004). *Reflectivity of Pavement Markings: Analysis of Retroreflectivity Degradation Curves.* (Report Number WA-RD 592.1). Washington State Transportation Center: University of Washington.

Korpela, I., Ørka, H.O. Hyyppä, J., Heikkinen, V., & Tokola, T. (2010). Range and AGC normalization in airborne discrete-return LIDAR intensity data for forest canopies. *ISPRS Journal of Photogrammetry and Remote Sensing*, *65*, 369–379.

Lazarus, J. (2012). *Aluminum Sign Recycling*. (Research Report SR500-510). Oregon Department of Transportation, Research Section. Retrieved from: https://www.oregon.gov/ODOT/Programs/ResearchDocuments/SR500_510_AlSigns.pdf

Li, Y., Fan, J., Huang, Y. & Chen, Z., (2016). Lidar-Incorporated Traffic Sign Detection from Video Log Images of Mobile Mapping System. *ISPRS-International Archives of the Photogrammetry, Remote Sensing and Spatial Information Sciences*, XLI-B1, 661-668.

Lloyd, J., (2008). *Understanding Retroreflectivity: A brief history of retroreflective sign face sheet materials*. Retrieved from https://www.rema.org.uk/pub/pdf/history-retroreflective-materials.pdf

Lundkvist, S.O. & Isacsson, U. (2007). Prediction of road marking performance. *Journal of Transportation Engineering*, 133(6), 341-346.

Luzum, B., Starek, M. & Slatton, K.C., (2004). *Normalizing ALSM intensities; Geosensing Engineering and Mapping (GEM) Center* (Report No. Rep_2004-07-01). Civil and Coastal Engineering Department, University of Florida, Gainesville, Florida.

Mallet, C. & Bretar, F. (2009). Full-waveform topographic lidar: State-of-the-art. *ISPRS Journal of Photogrammetry and Remote Sensing*, 64(1), 1-16.

McGee, H.W., & Taori, S. (1998). *Impacts on state and local agencies for maintaining traffic signs within minimum retroreflectivity guidelines*, (No. FHWA-RD-97-053). Department of Transportation, Federal Highway Administration.

Migletz, J., Graham, J., Bauer, K., & Harwood, D. (1999). Field surveys of pavement-marking retroreflectivity. *Transportation Research Record: Journal of the Transportation Research Board*, 1657, 71-78.

Mogelmose, A., Trivedi, M.M. & Moeslund, T.B., (2012). Vision-based traffic sign detection and analysis for intelligent driver assistance systems: Perspectives and survey. *IEEE Transactions on Intelligent Transportation Systems*, 13(4), 1484-1497.

Hunt, J.E., A. Vandervalk, and D. Snyder (2011). *Road Measurement System Evaluation, National Academies Press*, Washington, D.C.

Olsen, M.J., Roe, G.V., Glennie, C., Persi, F., Reedy, M., Hurwitz, D., Williams, K., Tuss, H., Squellati, A., & Knodler, M. (2013). "Guidelines for the use of mobile lidar in transportation applications," TRB NCHRP Final Report 748. https://www.trb.org/Publications/Blurbs/169111.aspx.

Oregon Department of Transportation (2002). Desired Conditions of Maintenance Features on State Highways.

Oregon Department of Transportation (2013a). Sign Inventory Database User's Guide.

Oregon Department of Transportation (2013b) Sign Inventory Database Field Handbook Guide.

Oregon Department of Transportation (2015a). Section 00170.85(c)(1): Responsibility for Defective Work of Part 00100, General Conditions, Oregon Standard Specifications for Construction.

Oregon Department of Transportation (2015b). Mobile Lidar. Retrieved from https://www.oregon.gov/ODOT/ETA/Pages/LiDAR.aspx

Oregon Department of Transportation (2018). Traffic Sign Design Manual. Retrieved from https://www.oregon.gov/ODOT/Engineering/Documents_TrafficStandards/Sign-Design-Manual.pdf

Pike, A., Hawkins Jr, H. & Carlson, P.J. (2007). Evaluating the retroreflectivity of pavement marking materials under continuous wetting conditions. *Transportation Research Record: Journal of the Transportation Research Board*, 2015, 81-90.

Pu, S., Rutzinger, M., Vosselman, G. & Elberink, S.O., (2011). Recognizing basic structures from mobile laser scanning data for road inventory studies. *ISPRS Journal of Photogrammetry and Remote Sensing*, 66(6), S28-S39.

Riveiro, B., Díaz-Vilariño, L., Conde-Carnero, B., Soilán, M. & Arias, P., (2016). Automatic Segmentation and Shape-Based Classification of RetroReflective Traffic Signs from Mobile LiDAR Data. *IEEE Journal of Selected Topics in Applied Earth Observations and Remote Sensing*, 9(1), 295-303.

Saetern, L.T., (2016). *Preliminary Investigation: Commercial Pavement Marking Management Systems.* Caltrans Division of Research, Innovation and System Information: https://www.dot.ca.gov/newtech/researchreports/preliminary_investigations/docs/commercial_pavement_marking_management_systems_pi.pdf

Sairam, N., Nagarajan, S. & Ornitz, S., (2016). Development of mobile mapping system for 3d road asset inventory. *Sensors*, 16(3), p.367.

Schaepman-Strub, G., Schaepman, M.E., Painter, T.H., Dangel, S. & Martonchik, J.V. (2006). Reflectance quantities in optical remote sensing—Definitions and case studies. *Remote Sensing of the Environment*, 103(1), 27-42.

Schnell, T., Aktan, F. & Lee, Y.C. (2003). Nighttime visibility and retroreflectance of pavement markings in dry, wet, and rainy conditions. *Transportation Research Record: Journal of the Transportation Research Board*, 1824, 144-155.

Shrestha, R., W. Carter, C. Slatton, C. & W. Dietrich, (2007). *"Research-Quality" Airborne Laser Swath Mapping: The Defining Factors. National Center for Airborne Laser Mapping (NCALM).* Retrieved from https://ncalm.cive.uh.edu/sites/ncalm.cive.uh.edu/files/files/publications/reports/NCALM_WhitePaper_v1.2.pdf

Soilán, M., Riveiro, B., Martínez-Sánchez, J. & Arias, P., (2016). Traffic sign detection in MLS acquired point clouds for geometric and image-based semantic inventory. *ISPRS Journal of Photogrammetry and Remote Sensing*, 114, 92-101.

Suykens, J.A. & Vandewalle, J., (1999). Least squares support vector machine classifiers. *Neural processing letters*, 9(3), 293-300.

Tan, M., Wang, B., Wu, Z., Wang, J. & Pan, G., (2016). Weakly Supervised Metric Learning for Traffic Sign Recognition in a LIDAR-Equipped Vehicle. *IEEE Transactions on Intelligent Transportation Systems*, 17(5), 1415-1427.

Vain, A., Kaasalainen, S., Pyysalo, U., Krooks, A. & Litkey, P. (2009). Use of naturally available reference targets to calibrate airborne laser scanning intensity data. *Sensors*, 9(4), 2780-2796.

Vu, A., Yang, Q., Farrell, J.A. & Barth, M., (2013), October. Traffic sign detection, state estimation, and identification using onboard sensors. In *16th International IEEE Conference on Intelligent Transportation Systems (ITSC 2013)*, 875-880. IEEE.

Wagner, W., Hyyppä, J., Ullrich, A., Lehner, H., Briese, C., & Kaasalainen, S. (2008). Radiometric calibration of full-waveform small-footprint airborne laser scanners. *Int. Arch. Photogramm. Remote Sens. Spat. Inf. Sci*, 37, 163-168.

Wen, C., Li, J., Luo, H., Yu, Y., Cai, Z., Wang, H. & Wang, C., (2016). Spatial-related traffic sign inspection for inventory purposes using mobile laser scanning data. *IEEE Transactions on Intelligent Transportation Systems*, *17*(1), 27-37.

Wu, S., Wen, C., Luo, H., Chen, Y., Wang, C. & Li, J., (2015), July. Using mobile LiDAR point clouds for traffic sign detection and sign visibility estimation. In *2015 IEEE International Geoscience and Remote Sensing Symposium (IGARSS)*, 565-568). IEEE.

Yang, B. & Dong, Z., (2013). A shape-based segmentation method for mobile laser scanning point clouds. *ISPRS journal of photogrammetry and remote sensing*, 81, 19-30.

Yang, B., Liu, Y., Dong, Z., Liang, F., Li, B. & Peng, X., (2017). 3D local feature BKD to extract road information from mobile laser scanning point clouds. *ISPRS Journal of Photogrammetry and Remote Sensing*, *130*, 329-343.

Yang, B., Dong, Z., Liu, Y., Liang, F. & Wang, Y., (2017). Computing multiple aggregation levels and contextual features for road facilities recognition using mobile laser scanning data. *ISPRS Journal of Photogrammetry and Remote Sensing*, *126*, 180-194.

Zhou, L. & Deng, Z., (2014), October. LIDAR and vision-based real-time traffic sign detection and recognition algorithm for intelligent vehicle. In *17th International IEEE Conference on Intelligent Transportation Systems (ITSC)*, 578-583. IEEE.